Available online at www.sciencedirect.com

ScienceDirect

Geochimica et Cosmochimica Acta 245 (2019) 327–351

Geochimica et Cosmochimica Acta

www.elsevier.com/locate/gca

Methane sources and sinks in continental sedimentary systems: New insights from paired clumped isotopologues $^{13}CH_3D$ and $^{12}CH_2D_2$

Thomas Giunta [a,*], Edward D. Young [b], Oliver Warr [a], Issaku Kohl [b], Jeanine L. Ash [b,1], Anna Martini [c], Scott O.C. Mundle [a,2], Douglas Rumble [d], Ileana Pérez-Rodríguez [e,f], Mark Wasley [d], Douglas E. LaRowe [e], Alexis Gilbert [g], Barbara Sherwood Lollar [a]

[a] Department of Earth Sciences, University of Toronto, Canada
[b] Department of Earth, Planetary and Space Sciences, University of California Los Angeles, USA
[c] Department of Geology and Environmental Studies, Amherst College, USA
[d] Geophysical Laboratory, Carnegie Institution of Washington, USA
[e] Department of Earth Sciences, University of Southern California, USA
[f] Earth and Environmental Science, University of Pennsylvania, USA
[g] Earth-Life Science Institute, Tokyo Institute of Technology, Japan

Received 17 April 2018; accepted in revised form 27 October 2018; Available online 8 November 2018

Abstract

Stable isotope compositions of methane ($\delta^{13}C$ and δD) and of short-chain alkanes are commonly used to trace the origin and fate of carbon in the continental crust. In continental sedimentary systems, methane is typically produced through thermogenic cracking of organic matter and/or through microbial methanogenesis. However, secondary processes such as mixing, migration or biodegradation can alter the original isotopic and composition of the gas, making the identification and the quantification of primary sources challenging. The recently resolved methane 'clumped' isotopologues $\Delta^{13}CH_3D$ and $\Delta^{12}CH_2D_2$ are unique indicators of whether methane is at thermodynamic isotopic equilibrium or not, thereby providing insights into formation temperatures and/or into kinetic processes controlling methane generation processes, including microbial methanogenesis.

In this study, we report the first systematic use of methane $\Delta^{13}CH_3D$ and $\Delta^{12}CH_2D_2$ in the context of continental sedimentary basins. We investigated sedimentary formations from the Southwest Ontario and Michigan Basins, where the presence of both microbial and thermogenic methane was previously proposed. Methane from the Silurian strata coexist with highly saline brines, and clumped isotopologues exhibit large offsets from thermodynamic equilibrium, with $\Delta^{12}CH_2D_2$ values as low as −23‰. Together with conventional $\delta^{13}C$ and δD values, the variability in $\Delta^{13}CH_3D$ and $\Delta^{12}CH_2D_2$ to first order reflects a mixing relationship between near-equilibrated thermogenic methane similar to gases from deeper Cambrian and Middle Ordovician units, and a source characterized by a substantial departure from equilibrium that could be associated with microbial methanogenesis. In contrast, methane from the Devonian-age Antrim Shale, associated with less saline porewaters, reveals $\Delta^{13}CH_3D$ and $\Delta^{12}CH_2D_2$ values that are approaching low temperature thermodynamic equilibrium. While microbial

* Corresponding author.
E-mail address: thomas.giunta@utoronto.ca (T. Giunta).
[1] Now at Rice University, USA.
[2] Now at University of Windsor, Canada.

https://doi.org/10.1016/j.gca.2018.10.030

methanogenesis remains an important contributor to the methane budget in the Antrim Shale, it is suggested that Anaerobic Oxidation of Methane (AOM) could contribute to reprocessing methane isotopologues, yielding $\Delta^{13}CH_3D$ and $\Delta^{12}CH_2D_2$ signatures approaching thermodynamic equilibrium.

Keywords: Methane; Clumped isotopologues; Sedimentary basins; Microbial methanogenesis; Anaerobic oxidation

1. INTRODUCTION

Unraveling methane sources and sinks is key to understanding carbon cycling over geological timescales. Although it has a relatively short residence time in the atmosphere, methane is an important greenhouse gas. By contrast, methane in the continental crust (e.g. in sedimentary systems or within crystalline rocks) has longer residence times due to the reducing nature of these environments as well as limited exchange with other reservoirs. In such crustal systems, three major methanogenesis pathways are considered: (i) 'thermogenic methane' resulting from the thermocatalytic cracking of longer chain hydrocarbons and organic matter (often associated with oil production in sedimentary basins), (ii) 'microbial methane' which can result from different type of metabolisms (e.g. CO_2 reduction, acetate fermentation), and in rare cases (iii) 'abiogenic methane' resulting from Sabatier-type reactions. The identification of these different pools and the resolution of potential mixing between them is traditionally explored using bulk stable isotopic compositions ($\delta^{13}C$ and δD) of the methane molecule, combined with the gas wetness ratio C_1/C_{2+} (e.g. Bernard et al., 1976; Schoell, 1988; Sherwood Lollar et al., 1993, 1994; Martini et al., 1996; Whiticar, 1999). Characterization of subsurface methane is strongly constrained by our ability to define these possible endmembers. Isotope ratios are key arbiters in this endeavor. In nature, the variability of reaction pathways, temperatures and isotopic compositions of substrates or chemical precursors can produce a wide spectrum of bulk methane isotopic compositions that can result in overlap in isotope space between different endmembers, making identification of the provenance of the methane challenging (e.g. Martini et al., 1998; Horita and Berndt, 1999; Etiope and Sherwood Lollar, 2013; Vinson et al., 2017).

Recent advances in mass spectrometry have allowed the measurement of multiply substituted clumped isotopologues (i.e. molecules with two or more heavy isotopes). This novel approach allows the investigation of isotope bond ordering in a molecule, which at thermodynamic equilibrium depends on the formation temperature of the molecule. For most molecules, the likelihood to produce a clumped, or multiply-substituted, isotopologue is enhanced with decreasing equilibrium temperature compared to a purely stochastic distribution (Wang et al., 2004; Eiler, 2007). Pioneer studies on clumped isotopologues were initiated on CO_2 molecules by measuring the rare abundance of $^{13}C^{18}O^{16}O$ in atmospheric CO_2 (Eiler and Schauble, 2004; Affek et al., 2007) or in carbonate samples (e.g. Ghosh et al., 2006; Ferry et al., 2011). Recently, Stolper et al. (2014a) – using high resolution mass spectrometry – and Ono et al. (2014) – using laser adsorption spectroscopy (TILDAS) – outlined methods to measure $^{13}CH_3D$, the more abundant of multiply substituted mass-18 clumped isotopologues of methane. The first application to natural samples by Stolper et al. (2014b) analyzed a series of gas samples from different sedimentary systems. While some of their samples were convincingly of thermogenic origin and others presumably affected by microbial activity, they suggested overall reasonably good agreement between temperatures calculated based on the relative abundance of $^{13}CH_3D$ with those occurring within the basin, demonstrating the role $^{13}CH_3D$ can play in determining formation temperature of methane within natural systems. Such good agreement between clumped-based temperatures and environmental temperatures was later supported by Stolper et al. (2015) in a detailed study of gases from the Antrim Shale (Michigan Basin), by Wang et al. (2015) for gas samples from sedimentary environments (Powder River Basin, North Cascadia margin) and from Precambrian cratonic rocks which are considered abiotic in origin (Sherwood Lollar et al., 2002), as well as by Douglas et al. (2016) in Arctic marine sediments. At the same time, both Stolper et al. (2015) and Wang et al. (2015) observed that laboratory methanogenic cultures or natural environments known to host methanogenic organisms, can produce methane with unrealistically higher clumped-based temperatures, and even in some cases, clear disequilibrium signatures (occurring when the abundance of a clumped isotopologue is lower than the stochastic distribution). These discrepancies between clumped-based temperatures and expected environmental temperatures were also correlated to large D/H disequilibrium between the methane and the water in which it was formed (Stolper et al., 2015; Wang et al., 2015; Douglas et al., 2016; Gruen et al., 2018). The potential for such large disequilibrium in some samples revealed a fundamental aspect of isotope bond (re-)ordering: in certain cases, methane is formed under thermodynamic equilibrium and the relative distribution of its isotopologues can be predicted and interpreted as an equilibrium temperature; in other cases, methane formation is controlled by kinetic effects yielding a distribution of isotopologues outside of equilibrium. This distinction between equilibrium and disequilibrium was also highlighted by Douglas et al. (2016) who observed a wide variability of clumped isotopologue signatures in a collection of gas seeps from Alaskan lakes, ranging from apparently thermogenic and equilibrated methane, to dramatically disequilibrated methane likely originating from methanogenic organisms, with many samples possibly resulting from mixing between these two 'pools'.

Nonetheless, the expression of such disequilibrium where microbial methanogenesis occurs is not always

clear-cut. For example, in the previously mentioned Antrim Shale, where gases have long been considered to be dominated by microbial methane (Martini et al., 1996, 1998, 2003; Waldron et al., 2007), samples interpreted to represent the most the microbial endmember appeared to be close to equilibrium with respect to environmental temperatures (Stolper et al., 2015). Seemingly equilibrated microbial methane has also been reported since then in other continental and marine sedimentary environments (Wang et al., 2015; Douglas et al., 2016; Inagaki et al., 2015; Ijiri et al., 2018). In order to reconcile these observations with laboratory-cultured methanogens (typically producing methane out of equilibrium), Stolper et al. (2015) proposed a model for microbial methanogenesis in which the degree of reversibility of the enzymatic reactions would allow methanogens to produce (near-)equilibrium methane. Accordingly, in the case of the Antrim Shale, Stolper et al. (2015) suggested extremely low substrate availability and slow formation rates would result in the production of near-equilibrated methane over geological timescales. The concept of a variable degree of reversibility was similarly put forward by Wang et al. (2015), who also proposed that methanogens in nature could produce a wide spectrum of clumped signatures, from disequilibrium to (near-) equilibrium, as a function of available free energy. Despite evidence for reversibility of the key enzyme involved in the methanogenesis pathway (Scheller et al., 2010), it is important to note that such near-equilibrium microbial methane has yet to be replicated under controlled (laboratory) conditions.

In the present study, we use the resolved relative concentrations of two rare mass-18 isotopologues, $^{12}CH_2D_2$ and $^{13}CH_3D$, as a sensitive indicator of the degree of thermodynamic equilibration of methane gas. The Matsuda-type large radius high-resolution mass spectrometer at UCLA has a mass resolving power ($> 40{,}000$) that allows the direct measurement of both $^{13}CH_3D$ and $^{12}CH_2D_2$. The latter is another mass-18 isotopologue of methane with extremely low abundance, typically $\sim$0.1 ppm (Young et al., 2016). This novel dimension has the potential to provide unambiguous formation temperatures of methane in cases where both clumped isotopologue systems yield consistent temperatures, and alternatively, sensitive indicators of kinetic and mixing processes where disequilibrium is indicated. We investigated $^{13}CH_3D$ and $^{12}CH_2D_2$ in natural gas samples from sedimentary strata of Cambrian, Ordovician and Silurian ages in the Southwest Ontario Basin (Canada), and from Silurian and Devonian age strata in the Michigan Basin (USA). The choice of these two geological settings is relevant for a first application of the two mass-18 isotopologues in continental sedimentary systems, because both systems are thought to host significant volumes of microbially derived methane (though under very different salinity regimes) in addition to thermogenic gases (Sherwood Lollar et al., 1993; Martini et al., 1996, 1998, 2003; Clark et al., 2015; Stolper et al., 2015). Furthermore, although Southwest Ontario Basin has been extensively explored and exploited for its hydrocarbon resources, questions remain with respect to the apparent low thermal maturity of the rocks (Barker and Pollock, 1984; Sherwood Lollar et al., 1994) and the significant production of light hydrocarbon gases (C_1, C_2, C_3...) implying more mature hydrocarbon generation, giving us an opportunity to provide additional constraints on the thermal history of this sedimentary system.

2. GEOLOGICAL AND GEOCHEMICAL BACKGROUNDS

2.1. Southwest Ontario and Michigan Basins

The Southwest Ontario Basin is a broad sedimentary platform that was deposited during intermittent marine transgression occurring from late Cambrian to Devonian era (Brigham, 1971; Johnson et al., 1992). The sedimentary succession lies on the Algonquin Arch, a Precambrian topographic high trending northeast-southwest, and separating two areas of major subsidence: the Michigan Basin to the northwest and the Appalachian Basin to the southeast (Fig. 1). The Algonquin Arch was formed during the late Precambrian and was occasionally reactivated during Paleozoic (Sanford et al., 1985). Southwest Ontario strata overlap to the north against the Precambrian basement and are rather flat-lying on the axis of the arch, with a total thickness of approximately 850 m.

In Southwest Ontario, the basal Cambrian unit, deposited on the Precambrian basement, has been extensively eroded during arch rejuvenation in the Early Paleozoic, explaining its absence from the sedimentary sequence in parts of Southwest Ontario. Cambrian strata consist of sandstone and dolomite, and can contain hydrocarbons (usually found in dolomitic pinchouts and in fault traps). Middle Ordovician strata overlie the Cambrian strata where it is present, and otherwise lie directly on the Precambrian basement. They are composed by two distinct limestone groups, the Black River group and the Trenton Group, the latter one being capped by the Upper Ordovician shale. These two groups host post-depositional hydrothermal dolomite mineralized adjacent to faults (Trevail et al., 2004) that likely extend from the Precambrian basement (Sanford et al., 1985; Carter et al., 1996). The timing for this hydrothermal fluid circulation is still debated and has been proposed to be of Silurian age according to Coniglio et al., (1994) (based on fluid inclusion thermometry) or of late Ordovician age according to Davies and Smith (2006) (based on SAG structures). In the Middle Ordovician limestones, the hydrothermal dolomite mineralization is thought to have increased local porosity and to serve as the primary reservoir for hydrocarbons (Davies and Smith, 2006). Above the Upper Ordovician shale, the Silurian strata consist of alternating dolostone and shale, with evaporitic units in the Upper Silurian. Hydrocarbons are also found in Silurian strata, with reservoirs resulting from permeability pinchouts. Lastly, the Devonian succession consists of interbedded dolostone, shale and limestone, with major oil and gas reservoirs found in the limestone units.

Due to their location on the topographic high of the Algonquin Arch, Southwest Ontario strata have been in a relatively moderate to low thermal regime. Based on con-

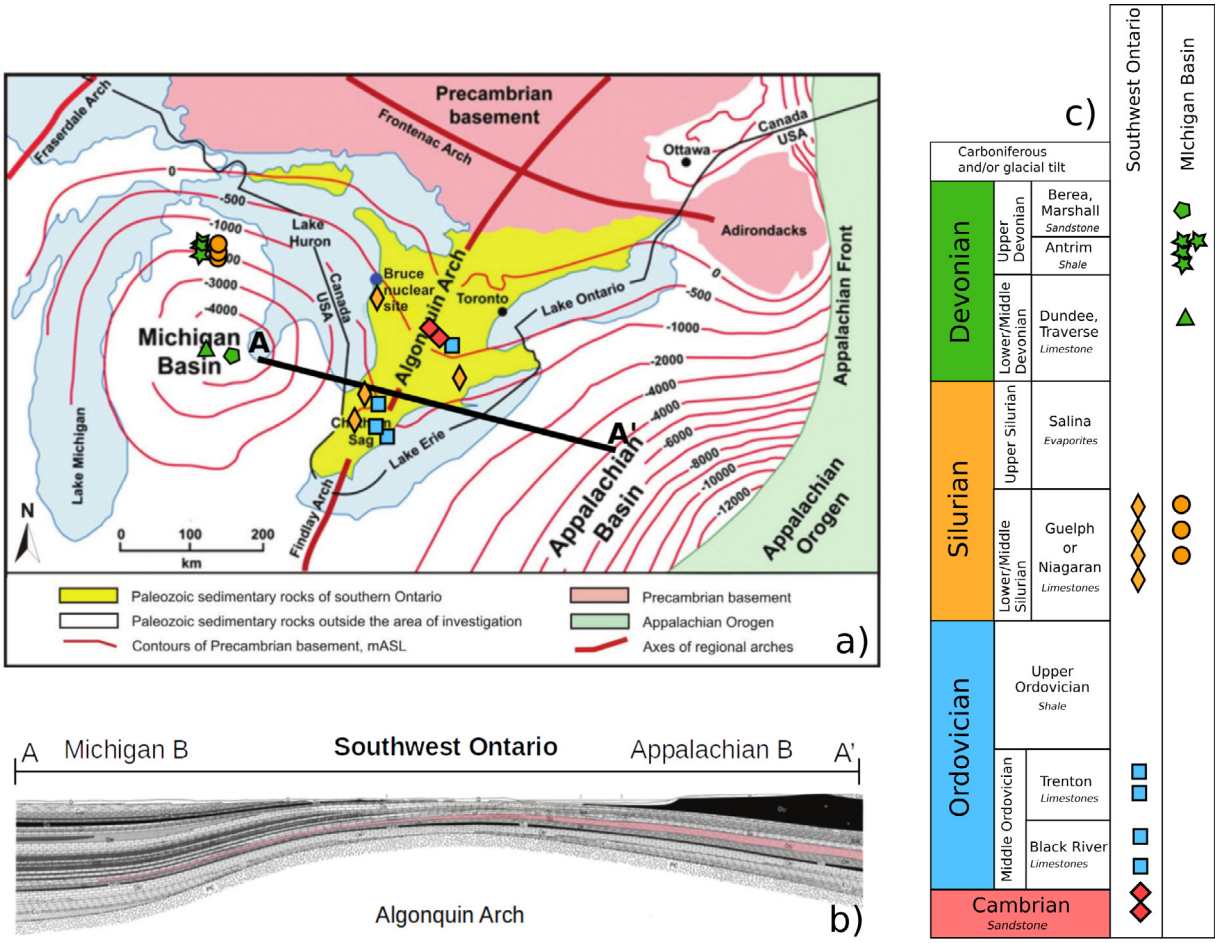

Fig. 1. Geological settings. (a) Structural map (modified after Mazurek, 2004) from Southwest Ontario (in yellow) overlying the Algonquin Arch, separating the Michigan Basin to the northwest, from the Appalachia Basin to the southwest. The location of the gases sampled and analyzed for their compositions in this study are also indicated. (b) Cross-section across the Algonquin Arch of Southwest Ontario (modified after Sanford, 1993). (c) Harmonized stratigraphic column in Southwest Ontario and in Michigan Basin (based on Armstrong and Carter, 2006; Ma et al., 2005). For easier comprehension, only the major and the sampled units have been represented in this figure. Note that the Niagaran unit in the Michigan Basin is stratigraphically equivalent to the Guelph unit in Southwest Ontario.

odont and acritarch alteration indices, Legall et al. (1981) distinguished two thermal facies in Paleozoic sections from Southwest Ontario. The first facies was identified from the top of the Devonian group down to the Trenton Group in the Middle Ordovician strata and indicated maximum burial temperature of only 60 °C. The second facies was identified from the Middle Ordovician to the base of the Paleozoic section and indicated a maximum burial temperature ranging between and 60 and 90 °C. In terms of hydrocarbon generation, these temperatures are considered to be immature to moderately mature (Legall et al., 1981; Obermajer et al., 1996). These apparently low burial temperatures contrast however with homogenization temperatures calculated from hydrothermal dolomite fluid inclusions which reach up to 220 °C in the Middle Ordovician units (Coniglio et al., 1994) and up to 130 °C in the Silurian units (Haeri-Ardakani et al., 2012). Resolving the thermal history of the basin has been a long-standing challenge.

By contrast to Southwest Ontario, marine incursions in the Michigan Basin, where much greater subsidence occurred, have accumulated up to 4500 m of sediments in the central part of the Basin (Dorr and Eschman, 1970). The Michigan Basin is composed of sediments ranging from Cambrian to Pennsylvanian-age, and contains a thick succession of Devonian sediments that include the organic-rich Antrim Shale. The Antrim Shale mostly consists of black shales interbedded with gray and green shales, as well as carbonate units (Gutschick and Sandberg, 1991). On the northern and the western margins of the Michigan Basin where it subcrops below glacial deposits, the Antrim Shale has accumulated natural gas of economic importance (Martini et al., 1996).

2.2. Gas and water geochemistry

Both Southwest Ontario and Michigan Basins contain light hydrocarbons (C_1, C_2, C_3...), of which methane is the major component (up to 90%). In Cambrian and Middle Ordovician strata from Southwest Ontario, investigations of carbon and hydrogen isotopic composition of light hydrocarbons ($^{13}C/^{12}C$ and D/H), suggests that these

gases are predominantly thermogenic in origin (Barker and Pollock, 1984; Sherwood Lollar et al., 1994), with formation temperatures possibly exceeding 200 °C based on $^{13}C/^{12}C$ relationships between ethane and propane (James, 1983; Sherwood Lollar et al., 1994). The Silurian limestones from Southwest Ontario are also reservoirs for thermogenic gases, sometimes oil-associated, but the progressive depletion in $\delta^{13}C$ and δD of the methane (Barker and Pollock, 1984) is thought to reflect the contribution of microbially derived methane (Sherwood Lollar et al., 1994; Clark et al., 2015).

In the Devonian Antrim Shale from the Michigan Basin, significant variations of C_1/C_{2+} (from 10 up to 10,000) were similarly proposed to reflect various degrees of mixing between thermogenic gases and a microbially derived methane, the latter possibly representing up to 80% of the total methane budget (Martini et al., 1996, 1998). Evidence for anaerobic oxidation of ethane and propane have led Martini et al. (1998, 2003) to suggest that a significant component of the methane in the Antrim Shale could be or could have been biodegraded as well. This hypothesis has been recently supported by the observation of methane consumption in Antrim Shale porewater incubations (Waldron et al., 2007; Wuchter et al., 2013), as well as by the identification of sulfate-reducing bacteria (Wuchter et al., 2013), which often co-exist with anaerobic methane oxidizers (Knittel and Boetius, 2009; Kirk et al., 2012).

While both Silurian strata from Southwest Ontario and the Antrim Shale from the Michigan Basin systems may contain significant volumes of microbially-derived methane (in addition to thermogenic gases), their salinity regimes are quite different. Indeed, the lower Paleozoic sections from Southwest Ontario, including the ones thought to contain microbial methane, are all associated with extremely saline brines, typically exceeding 250 g/L (Dollar et al., 1991; Hobbs et al., 2011; Skuce et al., 2015; Al et al., 2015). These saline brines show water isotopic compositions ($\delta^{18}O$ and δD) typical of evaporative brines in sedimentary systems (Knauth and Beeunas, 1986; Kharaka and Hanor, 2003) (see Fig. 2), and suggest negligible contribution of meteoric or glacial freshwater recharge in these formations (Hobbs et al., 2011). Although methanogens have been shown to grow at such high salinity (Oren, 2011; Zhilina et al., 2013), this observation led Clark et al. (2015) to suggest that microbial activity may have occurred in the geologic past before these fluids gained their salinity, and suggested the microbial component of methane found in Southwest Ontario is a 'relic' of a past microbial methanogenesis activity (Clark et al., 2015).

By contrast, porewaters from the Devonian Antrim Shale are impacted by the incursion of freshwater that followed Pleistocene glaciations (e.g. Martini et al., 1998, 2003; McIntosh and Walter, 2005; McIntosh et al., 2011, 2012). Such freshwater recharges, and the subsequent decrease of salinity, have been often proposed as a potential mechanism to enhance alkane biodegradation and late stage microbial methanogenesis in uppermost sedimentary formations from North American sedimentary basins (e.g. Martini et al., 1996, 1998; McIntosh et al., 2002).

3. MATERIAL AND METHODS

3.1. Gas sample collection

We collected a series (n = 10) of gas samples from Cambrian, Middle Ordovician and Middle Silurian strata in Southwest Ontario. In the Michigan Basin, we collected gas samples from the Devonian Antrim Shale (n = 4), as well as two samples from other Devonian formations (Dundee and Berea), and three samples from the Niagaran Silurian formation which is stratigraphically equivalent to the Silurian formation (Guelph) sampled in Southwest Ontario. In the Michigan Basin, we sampled gases from the Antrim Shale, as well as Devonian samples. All gases were sampled from economic gas wells and are summarized in Table 1, together with their locations and their geological formations.

In Southwest Ontario, samples for bulk isotope analyses ($\delta^{13}C$ and δD) and gas composition analyses (C_1, C_2, C_3...), were collected in pre-evacuated 160 mL glass vials fixed with $HgCl_2$ and sealed with blue butyl rubber stoppers after the method of Ward et al. (2004). Plastic tubing was connected to the wellhead and used to fill a large reservoir that can be sub-sampled. Prior to collecting the sample, gas was allowed to flow for approximately 10 min in order to flush out the reservoir and ensure a representative sampling. Gas was then sampled from the reservoir with a syringe and injected into the pre-evacuated vial. Some of the wells in Southwest Ontario were also sampled for mass-18 methane isotopologue measurements. For those, gases were collected in refrigeration-grade copper tubes (60 cm-long, 10 mm diameter), using the procedure developed and well-establish for noble gas and methane sampling (Sherwood Lollar and Ballentine, 2009). Typically, in order to sample several replicates, copper tubes are connected in series via plastic tubing connected to the wellhead. Here too the gas was allowed to flush for about 10 minutes before sampling to ensure a representative sample. Each copper tube is then successively crimped at both ends to ensure cold welding. Samples from the Michigan Basin also collected in copper tubes, using the same procedure as described above. For those, in addition to gas samples, water samples from the wellhead were also collected in order to measure water isotopic composition, ($\delta^{18}O$ and δD) as well as major chemistry. Water samples were not available when Southwest Ontario wells were sampled.

3.2. Gas composition measurement

Gas composition analyses were performed at the Stable Isotope Laboratory at the University of Toronto following methods presented by Ward et al. (2004) and Sherwood Lollar et al. (2006). Light hydrocarbons CH_4, C_2H_6, C_3H_8 and C_4H_{10} were measured on a Varian 3400 gas chromatograph equipped with a flame ionization detector (FID). Light hydrocarbons were separated on a J&W Scientific GS-Q column (30 m × 0.32 mm ID) with helium as carrier gas and temperature program following: 2.5 min at 60 °C then increasing to 120 °C at 5 °C/min. All analyses were run in triplicate and the reproducibility was ±5%.

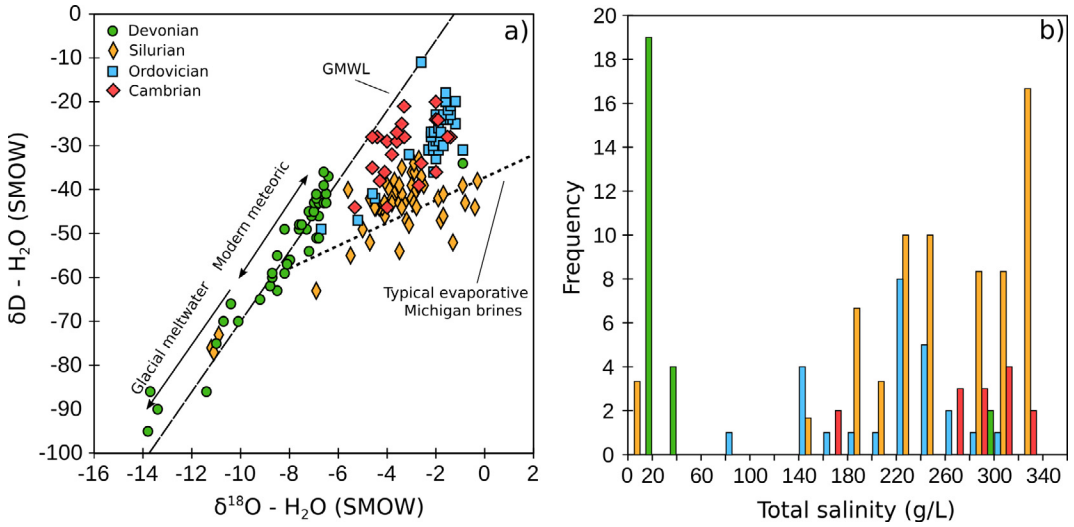

Fig. 2. Southwest Ontario porewater geochemistry. (a) The water isotopic composition ($\delta^{18}O$ and δD) is reported for porewaters from Devonian, Silurian, Ordovician and Cambrian strata. The GMWL refers to the Global Meteoric Water Line. The shallowest Devonian units show the clear influence of meteoric or glacial meltwater recharge, whereas Silurian, Ordovician and Cambrian porewaters are typically exhibiting an evaporative brine signature by plotting to the right of the GMWL with more elevated $\delta^{18}O$ and δD. (b) Histogram representing the distribution of the salinity (as Total Dissolved Solid) in g/L in porewaters from Southwest Ontario. With rare exception of samples collected at the northern part of Southwest Ontario, the Silurian, Ordovician and Cambrian strata are systematically showing extreme salinity. Data are from Dollar et al., (1991); Hobbs et al., (2011) and Skuce et al., (2015).

3.3. Methane isotopologues $^{12}CH_4$, $^{13}CH_4$, $^{12}CH_3D$, $^{13}CH_3D$ and $^{12}CH_2D_2$ measurements

Singly and doubly-substituted isotopologues of methane are measured on the Panorama, a prototype high resolution gas-source mass spectrometry developed by Nu Instruments at UCLA. The bulk carbon and hydrogen stable isotopic ratios are reported versus international standards (V-PDB and SMOW, respectively), and expressed in permil unit using the classic delta notation such as:

$$\delta^{13}C = \left[\left(^{13}C/^{12}C\right)_{sample}/\left(^{13}C/^{12}C\right)_{VPDB} - 1\right] \times 1000 \quad (1)$$

and

$$\delta D = \left[(D/H)_{sample}/(D/H)_{VSMOW} - 1\right] \times 1000 \quad (2)$$

Mass-18 isotopologue compositions are reported versus a stochastic distribution (Douglas et al., 2017 and reference therein), theoretically obtained at infinite temperature, and expressed in permil using the capital delta notation such as:

$$\Delta^{13}CH_3D = \left[\left(^{13}CH_3D/^{12}CH_4\right)_{sample}/\left(^{13}CH_3D/^{12}CH_4\right)_{stochastic} - 1\right] \times 1000 \quad (3)$$

and

$$\Delta^{12}CH_2D_2 = \left[\left(^{12}CH_2D_2/^{12}CH_4\right)_{sample}/\left(^{12}CH_2D_2/^{12}CH_4\right)_{stochastic} - 1\right] \times 1000 \quad (4)$$

The relationship between $\Delta^{13}CH_3D$ and $\Delta^{12}CH_2D_2$ and temperature can be predicted through *ab initio* calculations (e.g. Ma et al., 2008; Webb and Miller, 2014; Liu and Liu, 2016). In this study, we used the recent expressions proposed by Young et al., (2016, 2017):

$$\Delta^{13}CH_3D(T) \approx 1000\ln\left(1 + 0.0355502/T - 433.038/T^2 + 1270210.0/T^3 - 5.94804 \times 10^8/T^4 + 1.196630 \times 10^{11}/T^5 - 9.0723 \times 10^{12}/T^6\right) \quad (5)$$

and

$$\Delta^{12}CH_2D_2(T) \approx 1000\ln\left(1 + 0.183798/T - 785.483/T^2 + 1056280.0/T^3 + 9.37307 \times 10^7/T^4 - 8.919480 \times 10^{10}/T^5 + 9.901730 \times 10^{12}/T^6\right) \quad (6)$$

where T is in Kelvin. The differences between the different computational methods to predict relationship between Δ values and temperatures are less than the analytical uncertainties (Webb and Miller, 2014; Liu and Liu, 2016, Young et al., 2017). Accordingly, when methane is formed at thermodynamic equilibrium, $\Delta^{13}CH_3D$ and $\Delta^{12}CH_2D_2$ can only exhibit positive values that approach 0‰ at high temperatures (>1000 K).

Methods for sample purification and isotope ratio measurements are detailed by Young et al. (2016, 2017) and briefly summarized here. Prior to measurement of isotopologues, methane is purified on a vacuum line interfaced with a gas chromatograph (GC). In this study, copper tubes containing samples are mounted with a tube-piercer on the vacuum-line. The vacuum-line, including the piercer is pumped with a diaphragm rough pump, then with a turbo-molecular pump to a vacuum of $3 \cdot 10^{-5}$ mbar or better. The copper tube is then pierced and the gas transferred into a liquid nitrogen trap filled with silica-gel. Helium car-

Table 1
Gas samples collected and analyzed for their isotopic compositions. Errors (1σ) are ±0.1‰ and ±0.3‰ for methane $\delta^{13}C$ and δD respectively, ±0.3‰ for $\Delta^{13}CH_3D$, ±0.3‰ for $\Delta^{12}CH_2D_2$, ±1‰ for ethane and propane $\delta^{13}C$. nm = non measured. *State Charlton C4-31 was contaminated with air during samping.

Well name	Latitude	Longitude	Formation	Age	Methane (C_1)					Ethane (C_2)		Propane (C_3)		iC_4	nC_4	CO_2	
					% gas	$\delta^{13}C$	δD	$\Delta^{13}CH_3D$	$\Delta^{12}CH_2D_2$	% gas	$\delta^{13}C$	% gas	$\delta^{13}C$	% gas	% gas	% gas	$\delta^{13}C$
Southwest Ontario																	
Ram No. 33	42.70682	−82.34145	Guelph	Mid. Silurian	85.1	−54.3	−261	1.66	−20.17	5.5	−35.1	2.8	−28.6	1.1	0.7	<0.1	nm
Mesa Et Al Bemore No.1	43.87366	−81.46787	Guelph	Mid. Silurian	81.4	−49.3	−259	2.50	−14.65	5.1	−37.1	2.1	−30.7	1.5	0.4	<0.1	nm
Clearwood et al #12	43.57030	−81.49271	Guelph	Mid. Silurian	78.9	−46.9	−227	2.99	1.03	7.3	−36.3	3.4	−32.5	0.7	0.8	<0.1	nm
NOG #6	42.86167	−80.38750	Thorold	Mid. Silurian	79.9	−47.4	−281	3.39	−3.90	7.5	−39.9	2.9	−34.2	0.2	0.5	<0.1	nm
Ram/BP 4	42.27138	−82.13437	Trenton	Mid. Ordovician	83.8	−41.4	−199	2.96	9.07	6.3	−36.4	2.7	−34.1	0.3	0.6	<0.1	nm
PPC/RAM 29	42.36744	−82.35322	Trenton	Mid. Ordovician	64.3	−38.1	−180	2.59	8.94	5.9	−36.8	2.7	nm	0.3	0.7	<0.1	nm
Ram No. 84	42.64817	−82.28078	Black River	Mid. Ordovician	88.1	−40.8	−194	2.52	8.32	7.2	−33.9	3.4	−32.5	0.3	0.8	<0.1	nm
Cambright #80	43.23490	−80.53375	Black River	Mid. Ordovician	49.6	−41.9	−208	3.61	10.54	7.3	−36.1	1.4	−32.4	0.2	0.3	<0.1	nm
Cambright #63	43.35257	−80.91059	Camb./Black R.	Camb. /Mid. Ordo.	79.8	−38.4	−176	2.94	8.18	6.8	−33.1	3.1	−31.6	4.2	0.7	<0.1	nm
DGC #7 (Zehr Farms)	43.28426	−80.74963	Cambrian	Cambrian	78.6	−38.0	−174	2.45	6.18	8.1	−34.2	5.3	−31.7	1.0	2.0	<0.1	nm
Michigan Basin																	
North Charlton A1-18	45.08301	−84.48845	Antrim	Up. Devonian	93.8	−55.1	−270	5.58	13.83	0.2	−36.6	0.1	−30.9	0.0	0.0	5.91	12.0
State Charlton C4-31	44.94765	−84.47410	Antrim	Up. Devonian	43*	−52.7	−256	4.74	12.73	0.1*	nm	0.1*	nm	0.7*	0.0	nm	nm
Meunier D2-5	44.93099	−84.46496	Antrim	Up. Devonian	93.5	−53.8	−242	5.22	12.59	0.8	−45.1	0.1	−14.3	0.0	0.0	5.60	16.8
Terra Energy C3-8	44.91931	−84.46158	Up. Antrim	Up. Devonian	91.9	−54.1	−255	4.73	11.67	2.6	−45.5	0.1	−15.1	0.1	0.0	5.32	14.8
NWBU Berea	43.63273	−84.14695	Berea	Up. Devonian	41.5	−54.5	−330	3.90	−13.80	23.0	nm	24.3	nm	2.6	6.0	nm	nm
Dundee Gepford	43.65036	−84.76637	Dundee	Mid. Devonian	44.9	−53.6	−325	5.05	−11.09	33.7	−37.0	16.9	−31.0	1.8	2.8	<0.1	nm
State Chester	44.96016	−84.53597	Niagara	Mid. Silurian	59.6	−55.7	−308	1.53	−23.13	15.8	nm	12.8	nm	2.3	2.7	<0.1	nm
Gelow 2–13	44.92407	−84.50599	Niagara	Mid. Silurian	83.3	−55.1	−258	1.49	−17.34	8.8	−34.5	4.4	−29.8	1.9	1.7	<0.1	nm
Wesanen 2–19	44.98099	−84.47189	Niagara	Mid. Silurian	80.9	−54.0	−276	1.87	−17.11	10.5	−35.9	5.6	−30.9	1.3	1.6	<0.1	nm

rier gas is used to flush the sample to the GC as the trap is warmed at 30 °C. Two GC columns are used in series. The first column is used to separate H_2, Ar, O_2 and N_2, and consists of a 3-m long, 1/8-in. OD stainless steel tubing, packed with 5 A molecular sieve. The second column is used to separate CH_4 from other hydrocarbons, and consists of a 2-m long 1/8-in. OD stainless steel tubing packed with HayeSep D porous polymer. The helium flow-rate is set to ~20 mL/min and the temperature is fixed at 25 °C. Peaks are identified on a passive TCD, and retention time of methane is about 17 min. Methane is collected for 30 min in a second liquid nitrogen trap filled with silica-gel. Once methane collection is complete, the trap is slowly purged of helium at liquid nitrogen temperature, and then transferred to a glass vial filled with silica-gel as the trap is warmed up to 30 °C. This glass vial is then connected to the dual-inlet mass spectrometer and expanded into the sample variable-volume bellow as the silica-gel is heated up to 60 °C.

In order to measure $^{12}CH_4^+$, $^{13}CH_4^+$, $^{12}CH_3D^+$, $^{13}CH_3D^+$ and $^{12}CH_2D_2^+$ ion currents, the mass spectrometer is set to a mass resolving power equal or greater than 40,000. This allows the resolution of the two mass-18 isotopologues ($^{13}CH_3D$ and $^{12}CH_2D_2$), both measured on the axial collector with an electron multiplier. Meanwhile, mass-16 and mass-17 isotopologues are measured on Faraday collectors with amplifier resistors of 10^{11} Ω.

Sample and reference bellows are adjusted so that ion current intensities are balanced. First, the magnet is set to measure $^{12}CH_2D_2^+$ (18.04385 amu) on the axial collector, and $^{12}CH_3D^+/^{12}CH_4^+$ and $^{12}CH_2D_2/^{12}CH_4^+$ ratios are measured simultaneously. Typically, forty blocks composed of twenty 30 s sample/standard integration cycles are used to measure these ratios. In a second setting, the magnet is set to measure $^{13}CH_3D^+$ (18.04090 amu) on the axial collector, and $^{13}CH_4^+/^{12}CH_4^+$ and $^{13}CH_3D/^{12}CH_4^+$ ratios are measured simultaneously over twenty blocks of twenty 30 s integration cycles. The typical propagated internal errors for the calculation of $\Delta^{13}CH_3D$ and $\Delta^{12}CH_2D_2$ values are generally ±0.2‰ and ±0.6‰, respectively.

These methods and the accuracy of $\Delta^{13}CH_3D$ and $\Delta^{12}CH_2D_2$ measurements, as well as for $\delta^{13}C$ and δD, was assessed in the two previous publications by Young et al., (2016, 2017). Gases equilibrated from 300 to 600 °C facilitated by catalysts or produced through silane reactions all yielded $\Delta^{13}CH_3D$ and $\Delta^{12}CH_2D_2$ values in agreement with the theoretical relationship between isotopologue distribution and temperature. Overall, the external 1σ error (n = 22) including both the accuracy and the reproducibility is estimated to be ±0.3‰ for $\Delta^{13}CH_3D$, ±1‰ for $\Delta^{12}CH_2D_2$, ±0.1‰ for $\delta^{13}C$, and of approximately ±0.3‰ for δD.

3.4. Ethane and propane bulk isotope measurements

The carbon stable isotope ratios of ethane and propane were measured by gas chromatography-combustion-isotope ratio mass spectrometry (GC-C-IRMS) on a Finnigan MAT 252 interfaced with a Varian 3400 capillary GC following a method outlined in Ward et al. (2004). Hydrocarbons were separated by a Poroplot Q™ column (25 m × 0.32 ID) with the following temperature program: 40 °C during 1 min, then increase to 190 °C at 5 °C/min and hold for 5 min. The total error including accuracy and reproducibility was ±0.5‰ with respect to V-PDB standard.

3.5. Water geochemistry

At the time of the gas sample collection in Southwest Ontario, no water samples could be collected due to the gas field operations. However, the same sedimentary formations investigated in the present study were investigated for water geochemistry and isotopic composition in previous studies (Dollar et al., 1991; Hobbs et al., 2011; Skuce et al., 2015). For each collected gas from Southwest Ontario, we report in Table 2 the average of $\delta^{18}O$, δD, as well as the Total Dissolved Solid (TDS) measured in these same formations by previous studies. The reported 1σ represents the standard deviation of the mean. In the Michigan Basin, water samples were collected where possible. Major chemistry results and total dissolved solids (TDS) were measured at Amherst College, and $\delta^{18}O$ and δD were measured at the Environmental Isotope Laboratory, University of Waterloo. For those water samples, the 1σ represents the external error. Note that for two of the Niagaran gas samples (*Gelow 2-13* and *Wesanen 2-19*), it was not possible to sample the formation water. For these two, we used previously published data from Wilson and Long (1993).

3.6. Preparation of methanogens in laboratory

Methanogen cultures were prepared at Carnegie Institution of Washington as well as at University of Southern California following the methods described in Young et al. (2017). All strains were obtained from the Leibniz Institute DSMZ-German Collection of Microorganisms and Cell Cultures. *Methanococcus maripaludis* (DSM 14266; Jones et al., 1983) and *Methanococcus aeolicus* (DSM 17251; Kendall et al., 2006) were grown in a crimped serum bottles with a ratio of headspace to culture volume of 70:7 mL in a base medium containing (L^{-1} distilled water): KH_2PO_4 (0.14 g), NH_4Cl (0.25 g), KCl (0.34 g), $MgCl_2.6H_2O$ (4.0 g), $CaCl_2.2H_2O$ (0.14 g), $NaHCO_3$ (5.0 g), NaCl (18.0 g), $Fe(NH_4)_2(SO_4)_2{\cdot}6H_2O$ (2.0 mg), resazurin (1.0 mg), 10 mL of trace-element solution 141 (Balch et al., 1979) and 10 mL of vitamin solution (Wolin et al., 1963). The medium was prepared anaerobically under H_2/CO_2 (80:20) with $Na_2S{\cdot}9H_2O$ (0.5 g/L) as the reducing agent. The pH of the medium was adjusted to 7.0. Batch reactions at 2 bar absolute pressure were incubated under optimal temperature conditions of 37 °C and 46 °C, respectively. Single un-inoculated serum vials, incubated along with the cultures at 37 °C and 46 °C, were used as negative controls. *Methanosarcina barkeri* (DSM 800) strain was grown under CH_3OH (methylotrophic pathway) at 37 °C in a base medium containing (L^{-1} distilled water): K_2HPO_4 (0.35 g), KH_2PO_4 (0.23 g), NH_4Cl (0.50 g), $MgSO_4.7H_2O$ (0.50 g), $CaCl_2.2H_2O$ (0.25 g), NaCl (2.25 g), 2 mL of $FeSO_4{\cdot}7H_2O$ solution (0.1% w/v in 0.1 H_2SO_4), 1 mL of trace-element solution SL-10 (Widdel

Table 2
Porewater geochemistry associated with the same economic gas wells from which gas samples in Table 1 were collected. For samples with an asterisk (*), we average previously published data from literature from the same geological unit (Hobbs et al., 2011; Skuce et al., 2015; Wilson and Long, 1993).

Well name	Formation	Age	δD (VSMOW)	±1σ	$\delta^{18}O$ (VSMOW)	±1σ	TDS (g/L)	±1σ	ε (m/w)
Southwest Ontario									
Ram No.33	Guelph	Mid. Silurian	−41.3*	4.3	−2.8*	3.3	300.0*	48.2	−229.4
Mesa Et Al Bemore No.1	Guelph	Mid. Silurian	−41.3*	4.3	−2.8*	3.3	300.0*	48.2	−227.0
Clearwood et al #12	Guelph	Mid. Silurian	−41.3*	4.32	−2.8*	3.26	300.0*	48.2	−193.8
NOG #6	Thorold	Mid. Silurian	−42.1*	6.2	−3.0*	1.0	218.8*	75.8	−249.7
Ram/BP 4	Trenton	Mid. Ordovician	−30.1*	7.7	−2.0*	0.7	211.3*	48.0	−174.1
PPC/RAM 29	Trenton	Mid. Ordovician	−30.1*	7.7	−2.0*	0.7	211.3*	48.0	−154.9
Ram No. 84	Black River	Mid. Ordovician	−30.1*	7.7	−2.0*	0.7	211.3*	48.0	−169.3
Cambright #80	Black River	Mid. Ordovician	−30.1*	7.7	−2.0*	0.7	211.3*	48.0	−183.0
Cambright #63	Camb./Black R.	Camb. /Mid. Ordo.	−28.9*	4.3	−3.6*	1.0	279.7*	48.4	−151.3
DGC #7 (Zehr Farms)	Cambrian	Cambrian	−28.9*	4.3	−3.6*	1.0	279.7*	48.4	−149.8
Michigan Basin									
North Charlton A1-18	Antrim	Up. Devonian	−89.3	2.5	−13.3	0.5	10.2	0.5	−198.9
State Charlton C4-31	Antrim	Up. Devonian	−77.3	2.5	−12.8	0.5	47.2	2.4	−193.9
Meunier D2-5	Antrim	Up. Devonian	−61.7	2.5	−9.3	0.5	85.9	4.3	−192.5
Terra Energy C3-8	Up. Antrim	Up. Devonian	−76.8	2.5	−12.1	0.5	86.8	4.3	−193.4
NWBU Berea	Berea	Up. Devonian	−24.6	2.5	−1.4	0.5	255.8	12.8	−313.1
Dundee Gepford	Dundee	Mid. Devonian	−34.2	2.5	−2.6	0.5	185.7	9.3	−300.8
State Chester	Niagara	Mid. Silurian	−79.8	2.5	−12.1	0.5	92.7	4.6	−248.3
Gelow 2–13	Niagara	Mid. Silurian	−40.2*	7.5	−0.3*	1.90	351.2*	63.2	−226.4
Wesanen 2–19	Niagara	Mid. Silurian	−40.2*	7.5	−0.3*	1.90	351.2*	63.2	−245.6

et al., 1983), yeast extract (2.0 g), casitone (2.0 g), 0.50 mL of Na-resazurin solution (0.1% w/v), $NaHCO_3$ (0.85 g), CH_3OH (5 ml), $Na_2S.9H_2O$ (0.30 g), L-cysteine-HCl × $7H_2O$ (0.30 g) and 10 mL of vitamin solution (Wolin et al., 1963). Medium was prepared anaerobically under N_2/CO_2 (80:20) and with a final pH of 6.5–6.8. CH_4 produced during culturing was extracted from the serum bottles using a gas-tight syringe and purified on the vacuum line to remove water vapor and any other headspace gases.

4. RESULTS

4.1. Methane in Southwest Ontario

Gases from Southwest Ontario strata are predominantly composed of methane (40–90%), with variable amounts of ethane (2–21%) and propane (1–11%), as well as nitrogen (up to 15%). These gases show relatively homogeneous C_1/C_{2+} ratios, usually between 5 and 10 (average is 7 ± 3). In this set of samples, methane exhibits significant variation in isotopic composition, ranging from −54‰ to −37‰ in $\delta^{13}C$, and from −281 to −172‰ in δD (Table 1). A general observation is that deeper Cambrian and Ordovician gases are isotopically more enriched in ^{13}C and D than methane found in the Silurian formations. When isotopic compositions are reported in a conventional 'Schoell plot' (Fig. 3a), Cambrian and Ordovician gases plot in a region typical of thermogenic gases, while gases from the Silurian strata are more ambiguous and could be either interpreted as low thermal maturity gases (Schoell, 1988; Hunt, 1996; Etiope et al., 2009), or as methane deriving from microbial methanogenesis, or as mixtures with these two sources. The range of isotopic variations observed here, together with the broad positive correlation between $\delta^{13}C$ and δD, are similar to previously published data on Southwest Ontario hydrocarbon gases (Sherwood Lollar et al., 1994; Clark et al., 2015).

Samples that were measured for clumped isotopologues cover the full range from most depleted to most enriched bulk isotope composition, and are reported in Fig. 3c in a $\Delta^{13}CH_3D$ versus $\Delta^{12}CH_2D_2$ diagram. In this doubly-substituted isotopologue space, methane at internal equilibrium should fall on the equilibrium curve, where both isotopologues indicate the same formation temperature (calculated using equations in Section 3.3). Cambrian and Ordovician gases typically plot on the equilibrium curve within error. Converting $\Delta^{13}CH_3D$ and $\Delta^{12}CH_2D_2$ into formation temperatures (Table 3), these gases appear to have been equilibrated at temperatures ranging between 110 °C and 204 °C. By contrast, methane from the Silurian formations exhibit large disequilibrium, displaced from the equilibrium curve toward very negative $\Delta^{12}CH_2D_2$ values as low as −23‰. Although there are only four Silurian samples for Southwest Ontario, the degree of disequilibrium seems to be related to the degree of depletion in bulk δD (Fig. 3a).

Fig. 4 shows the clumped compositions versus the D/H fractionation between methane and water from the same formations. This type of diagram was previously used by Stolper et al. (2015) and Wang et al. (2015) to distinguish methane samples formed at equilibrium, by investigating whether the fractionation between methane and water corresponded to equilibrium at the temperature inferred from

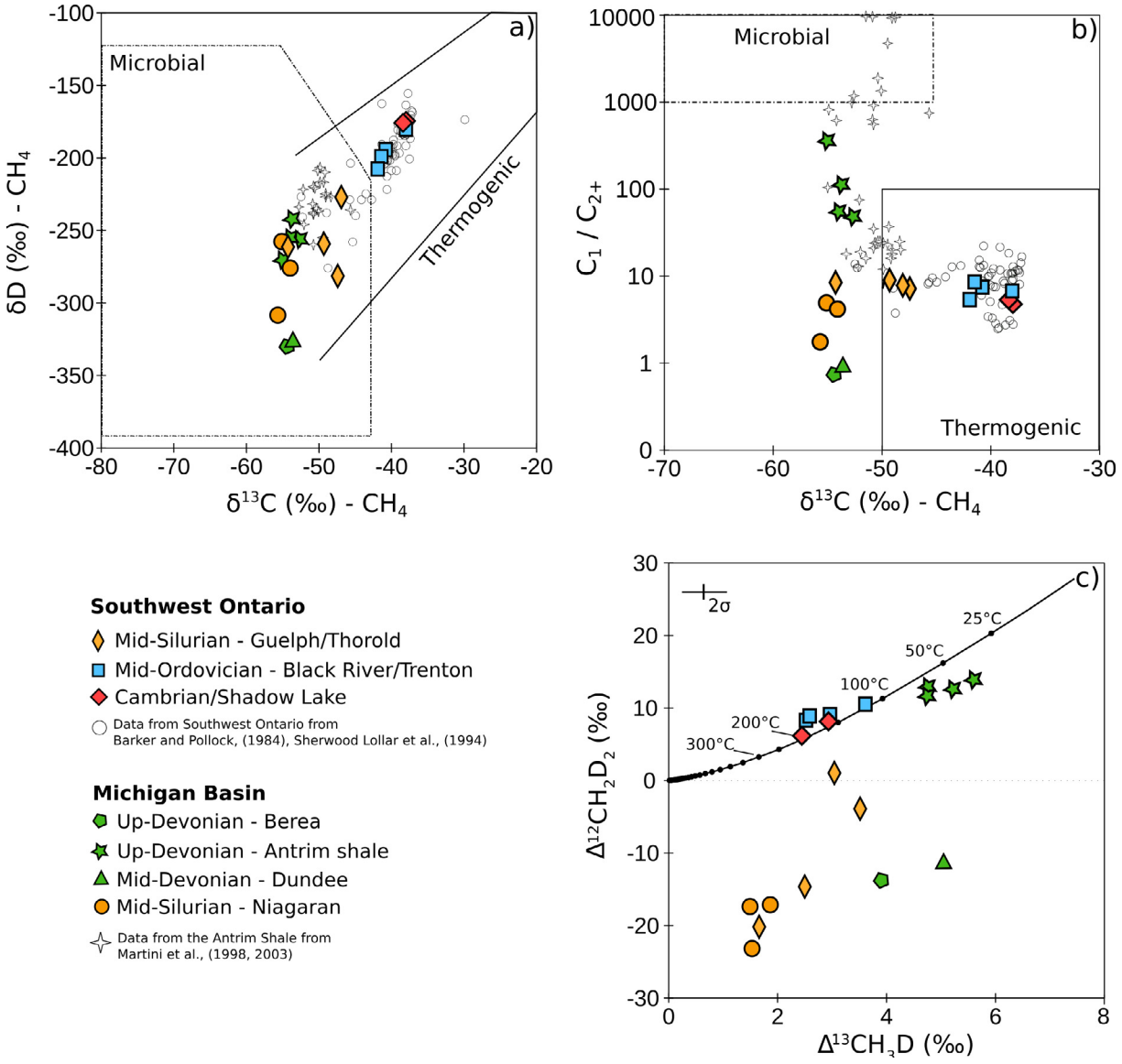

Fig. 3. Composite figure of results from Table 1. (a) $\delta^{13}C$ versus δD in a 'Schoell plot' (using microbial and thermogenic ranges as defined by Schoell, 1988; Sherwood Lollar et al., 2006). The range of variation measured in this study are in agreement with previous studies in Southwest Ontario (Barker and Pollock, 1984; Sherwood Lollar et al., 1994), or in the Antrim Shale (Martini et al., 1998). (b) Conventional 'Bernard plot' reporting $\delta^{13}C$ versus $C_1/(C_2+C_3)$ and microbial and thermogenic ranges. Southwest Ontario exhibit a relatively narrow range of variation in $C_1/(C_2+C_3)$, but significant variations in $\delta^{13}C$. By contrast, gases from the Michigan Basin exhibit a relatively narrow range of variation for $\delta^{13}C$, but wide variations of $C_1/(C_2+C_3)$ (particularly in the Antrim Shale), in all cases shown in light grey. (c) Clumped isotopologue space illustrates whether methane is at internal thermodynamic equilibrium (black line) or not. The thermodynamic equilibrium curve is calculated following Eqs. (1) and (2) (after the method of Young et al., 2016).

$\Delta^{13}CH_3D$. We note though that this equilibrium identification method implicitly assumes that the methane and the water are co-genetic, and does not consider that gases and water might have distinct sources and/or migration pathways. Here however, samples that are close to internal equilibrium with respect to mass-18 compositions (Cambrian and Ordovician gases), also appear near equilibrium with respect to D/H fractionation between methane and water. By contrast, Silurian gases show disequilibrium in both $\Delta^{13}CH_3D$ and $\Delta^{12}CH_2D_2$ space (Fig. 3c) and in the D/H fractionation (Fig. 4a and b).

4.2. Methane in the Michigan Basin

Gas samples from the Michigan Basin are also predominantly composed of methane. However, in contrast to the Southwest Ontario gases, these gases are highly variable in the C_1/C_{2+} ratios with values ranging from less than 1 in the Dundee and Berea formations up to 355 in the Antrim Shale (Fig. 3b). Significant variability of the C_1/C_{2+} in the Antrim Shale formation was also observed in previous studies (e.g. Martini et al., 2003) and attributed to a combination of microbial methanogenesis and anaerobic

Table 3
Apparent temperatures calculated (when possible) from $\Delta^{13}CH_3D$ and $\Delta^{12}CH_2D_2$.

Well name	Age	$\Delta^{13}CH_3D$	T (°C)	+/−	$\Delta^{12}CH_2D_2$	T (°C)	+/−
Southwest Ontario							
Ram No.33	Mid. Silurian	1.66	298	+52/−40	−20.17	nr	
Mesa Et Al Bemore No.1	Mid. Silurian	2.50	200	+30/−26	−14.65	nr	
Clearwood et al #12	Mid. Silurian	2.99	159	+24/−21	1.03	533	+1217/−145
NOG #6	Mid. Silurian	3.39	131	+21/−18	−3.90	nr	
Ram/BP 4	Mid. Ordovician	2.96	161	+24/−21	9.07	132	+17/−16
PPC/RAM 29	Mid. Ordovician	2.59	192	+28/−25	8.94	134	+18/−16
Ram No. 84	Mid. Ordovician	2.52	198	+30/−26	8.32	145	+19/−17
Cambright #80	Mid. Ordovician	3.61	118	+19/−17	10.54	110	+14/−13
Cambright #63	Camb./Mid. Ordo.	2.94	163	+24/−22	8.18	147	+20/−17
DGC #7 (Zehr Farms)	Cambrian	2.45	204	+31/−26	6.18	191	+28/−24
Michigan Basin							
North Charlton A1-18	Up. Devonian	5.58	31	+10/−10	13.83	72	+10/−10
State Charlton C4-31	Up. Devonian	4.74	62	+13/−12	12.73	83	+11/−11
Meunier D2-5	Up. Devonian	5.22	43	+12/−10	12.59	85	+11/−11
Terra Energy C3-8	Up. Devonian	4.73	62	+13/−12	11.67	95	+13/−11
NWBU Berea	Up. Devonian	3.90	101	+17/−15	−13.80	nr	
Dundee Gepford	Mid. Devonian	5.05	50	+11/−11	−11.09	nr	
State Chester	Mid. Silurian	1.53	320	+57/−45	−23.13	nr	
Gelow 2–13	Mid. Silurian	1.49	326	+59/−46	−17.34	nr	
Wesanen 2–19	Mid. Silurian	1.87	270	+43/−37	−17.11	nr	

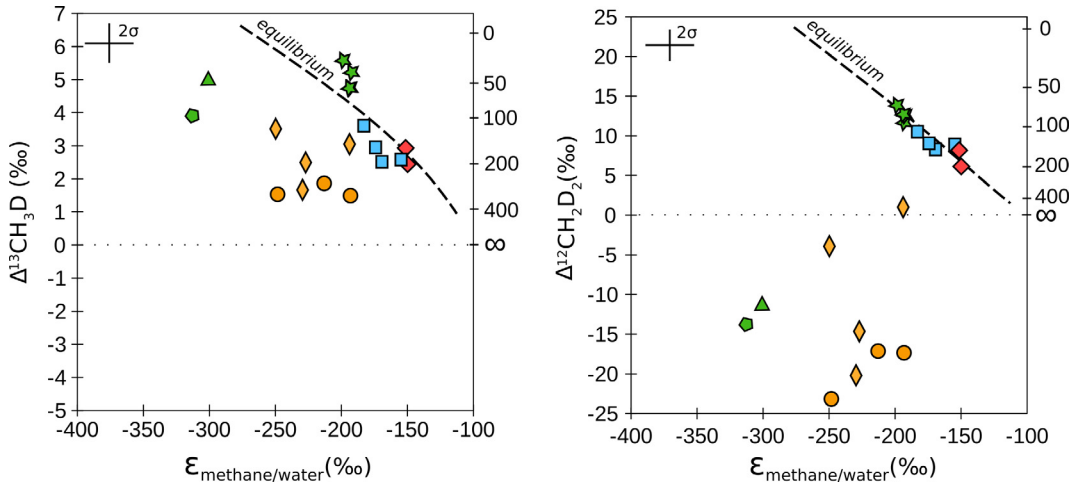

Fig. 4. $\Delta^{13}CH_3D$ and $\Delta^{12}CH_2D_2$ plotted versus the fractionation between methane and associated formation waters. This fractionation is reported as ε (as in Wang et al., 2015). The equilibrium curve is calculated using Horita and Wesolowski (1994) and Horibe and Craig (1995) calibrations. For Southwest Ontario, no water samples could be collected at the time of gas collection, hence average values of water samples collected and measured in previous studies (Hobbs et al., 2011) in the same formations are used (see Table 2). Symbols as in Fig. 3.

oxidation of hydrocarbons. Compared to Southwest Ontario, $\delta^{13}C$ of methane appears relatively homogeneous, with values ranging between −53 and −56‰. By contrast, δD of methane shows greater variability, with values ranging from −242‰ to −330‰. In a 'Schoell' plot, all samples from the Michigan Basin plot in the region where thermogenic gases and microbial gases overlap (Fig. 3a).

In terms of clumped compositions, these Michigan Basin samples plot in two distinct fields on the $\Delta^{13}CH_3D$ versus $\Delta^{12}CH_2D_2$ diagram (Fig. 3c). The four Antrim Shale samples all plot slightly below the equilibrium curve with values for $\Delta^{13}CH_3D$ and for $\Delta^{12}CH_2D_2$ ranging between 4.7 and 5.6‰, and between 11.7 and 13.8‰, respectively. Importantly, two of the Antrim Shale wells (*North Charlton A1-18* and *State Charlton C4-31*) were previously sampled by Stolper et al. (2015) who reported $\Delta^{13}CH_3D$ values in good agreement with our measurements. These are the first reported values for $\Delta^{12}CH_2D_2$. By contrast, the three samples from the Silurian Niagaran unit, and the two samples from the Devonian unit (Dundee and Berea) show significant deviations from the equilibrium curve, comparable in magnitude to that observed in Silurian samples from Southwest Ontario.

When $\Delta^{13}CH_3D$ and $\Delta^{12}CH_2D_2$ are reported versus D/H fractionation between methane and water (Fig. 4a and b), samples that are in disequilibrium with respect to clumped isotopologues are also in disequilibrium for D/H (Silurian, and Devonian Dundee and Berea). The exception are the samples from the Antrim Shale. Those which showed approximate equilibrium in the $\Delta^{13}CH_3D$ and $\Delta^{12}CH_2D_2$ plot (Fig. 3c) are also at near-equilibrium for D/H fractionation, suggesting that methane in the shale formation was formed or re-processed towards equilibrium with the porewaters.

4.3. Methanogen cultures

Methane produced during laboratory cultures of *Methanococcous maripaludis, Methanococcus aeolicus* and *Methanosarcina barkeri* shows important departures from the mass-18 isotopologue equilibrium curve (**see** Table 4 and Fig. 5). Those disequilibrium values, and the fact that $\Delta^{12}CH_2D_2$ is systematically more fractionated than $\Delta^{13}CH_3D$ are consistent with previous observations by Young et al. (2017), and attributed to the expression of large kinetic isotope effects during microbial methanogenesis. The negative $\Delta^{12}CH_2D_2$ seems to be typical of microbial methanogenesis. Notably, with the exception of two Sabatier experiments producing abiotic methane (Young et al., 2017), the methane produced by *Methanosarcina barkeri* exhibits one of the most depleted $\Delta^{12}CH_2D_2$ value measured so far ($\Delta^{12}CH_2D_2 = -55.3‰$). More dedicated studies are required to better constrain controls on the extent of kinetic effects during microbial methanogenesis and abiotic organic synthesis. However, based on the six species investigated so far, a pattern may be emerging whereby the CO_2-reduction pathway ($HCO_3^{2-} + 4H_2 + H^+ \rightarrow CH_4 + H_2O$) results in a smaller degree of disequilibrium compared to the methanol fermentation pathway ($4CH_3OH \rightarrow 3CH_4 + CO_2 + 2H_2O$), for both $\Delta^{13}CH_3D$ and $\Delta^{12}CH_2D_2$.

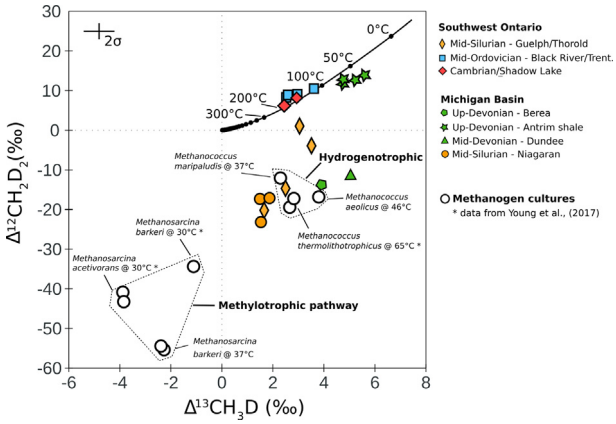

Fig. 5. We report the clumped isotopologue composition produced by 3 strains of methanogens, in addition to the one already published by Young et al. (2017). Natural gas samples measured in this study are also reported. The methane produced in laboratory cultures systematically carries large clumped disequilibrium, which is consistent with observed in previous studies for $\Delta^{13}CH_3D$ (Stolper et al., 2015; Wang et al., 2015; Young et al., 2017; Gruen et al., 2018) and for $\Delta^{12}CH_2D_2$ (Young et al., 2017). These large disequilibria are thought to reflect primary and secondary kinetic isotope effects during reduction and hydrogenation of carbon (Stolper et al., 2015; Wang et al., 2015), as well as quantum tunneling or combinatorial effects (Young et al., 2017).

5. DISCUSSION

5.1. Thermogenic, near-equilibrium methane, in Cambrian and Ordovician strata

Samples from the Cambrian and the Ordovician strata in Southwest Ontario plot on, or slightly above the equilibrium curve **(**Fig. 3**c)**, reflecting temperatures (between 110 °C and 205 °C – see Table 3) that are consistent with what is considered to be the typical thermogenic 'gas window' (Tissot and Welte, 1978). The isotopic composition of these gases, between −38 and −42‰ for $\delta^{13}C$, and between −174 and −207‰ for δD, are also in agreement with a thermogenic origin (e.g. Whiticar, 1999). Although the thermogenic generation of light hydrocarbons (including methane) is generally discussed in terms of kinetics isotope effects (e.g. Clayton, 1991; Lorant et al., 1994; Tang et al., 2000; Xia and Gao, 2017), this novel dataset which combines both $\Delta^{13}CH_3D$ and $\Delta^{12}CH_2D_2$, adds further support to the hypothesis made by Stolper et al. (2014b) proposing that thermogenic methane was generally at internal isotopic equilibrium with its formation temperature. Indeed, with few exceptions in unconventional gas reservoirs (Douglas et al., 2017; Stolper et al., 2017), the vast majority of thermogenic gases found in natural reservoirs or deriving from pyrolysis experiments (with one exception, see following section) yield clumped compositions in agreement with internal equilibrium (Stolper et al., 2014b, 2015, 2017; Wang et al., 2015; Douglas et al., 2016, 2017; Young et al., 2017).

The fact that Cambrian and Ordovician gases appear to be dominantly of thermogenic origin is consistent with previous studies on these formations (Barker and Pollock,

Table 4
Isotopic composition of methane produced in laboratory cultures by various strains of methanogens using two different set of substrates.

Methanogen strain	T (°C)	Substrate	$\delta^{13}C$ (VPDB)	δD (VSMOW)	$\Delta^{13}CH_3D$	$\Delta^{12}CH_2D_2$
Methanococcus aeolicus	46	CO_2/H_2	−53.2	−390.9	2.83	−17.34
Methanococcus aeolicus	46	CO_2/H_2	−51.5	−399.6	3.80	−16.94
Methanococcus maripaludis	37	CO_2/H_2	−50.3	−372.6	2.30	−12.11
Methanosarcina barkeri	37	CH_3OH	−53.7	−250.1	−2.37	−54.49
Methanosarcina barkeri	37	CH_3OH	−53.4	−249.9	−2.26	−55.34

1984; Sherwood Lollar et al., 1994). At this stage though, it is difficult to evaluate if the apparent temperature gradient derived from mass-18 isotopologues (from 110 °C to 205 °C) reflects a maturity trend (which would be consistent with increasing bulk heavy/light isotope ratios – see Table 1), or if it reflects mixing between two thermogenic sources. As previously mentioned, the abundant presence of thermogenic gases in Southwest Ontario strata was considered enigmatic, given thermal estimates based on Conodonts Alteration Index suggesting that the thermal burial regime experienced by the Paleozoic strata was at most 60–90 °C (Legall et al., 1981; Obermajer et al., 1996). The higher temperatures inferred from ethane and propane $\delta^{13}C$ relationship (Sherwood Lollar et al., 1994), and confirmed here with clumped isotopologues, are remarkably similar to homogenization temperatures of fluid inclusions found in hydrothermal dolomites throughout Ordovician strata (Coniglio et al., 1994; Haeri-Ardakani et al., 2012). Those fluids inclusions, which sometimes contain traces of hydrocarbons, record temperatures ranging between 100 and 220 °C, thus covering the range of temperatures inferred from $\Delta^{13}CH_3D$ and $\Delta^{12}CH_2D_2$. This supports a scenario in which thermogenic generation and migration of hydrocarbons in Southwest Ontario is closely related to the circulation of hydrothermal fluids estimated to have occurred between 350 Myrs (Haeri-Ardakani et al., 2012) and 440 Myrs ago (Davies and Smith, 2006). Those warm dolomitizing fluids likely originated from deeper environments in the Michigan or in the Appalachian Basin (both have experienced greater burial temperatures) and have been suggested to have circulated through the permeable Cambrian aquifer before infiltrating Ordovician through vertical fractures (Davies and Smith, 2006). Overall, this would indicate a long-term preservation of fluids and gases in Cambrian and Ordovician units. This conclusion is in agreement with the accumulation of radiogenic helium observed in this units, which suggests that the fluids have been isolated for more than 260 Myrs (Clark et al., 2013).

In the plot of $\Delta^{13}CH_3D$ or $\Delta^{12}CH_2D_2$ versus D/H fractionation between methane and water, Cambrian and Ordovician gases also plot on or near the equilibrium curve (see Fig. 4a and b). This indicates that the measured D/H fractionation between methane and water is close to equilibrium for temperatures similar to the one recorded by $\Delta^{13}CH_3D$ and $\Delta^{12}CH_2D_2$ and could suggest methane and water in these formations are co-genetic. In addition, the fact that neither clumped isotopologue, nor methane and water D/H fractionations have re-equilibrated with the current lower temperatures of these formations (<40 °C), supports the idea that the methane 'blocking temperature' (below which rates of isotope exchange are too low for significant re-equilibration) is >200 °C, consistent with the temperature limit proposed by Stolper et al. (2014b, 2017) or Wang et al., (2018).

5.2. Large disequilibrium in laboratory cultures and Silurian and Devonian strata

All methane samples from laboratory cultures exhibit strong disequilibrium, characterized by significant depletions in $\Delta^{13}CH_3D$ and $\Delta^{12}CH_2D_2$ compared to growth temperatures (Table 4 and Fig. 5). This dataset confirms that the $\Delta^{13}CH_3D$ disequilibria previously observed in laboratory cultures (Stolper et al., 2015; Wang et al., 2015; Douglas et al., 2016; Young et al., 2017; Gruen et al., 2018), are associated with even larger $\Delta^{12}CH_2D_2$ offsets from equilibrium (Young et al., 2017). Here, it is also remarkable that methane produced through the methylotrophic pathway (i.e. from methanol fermentation) seems to be associated with larger disequilibrium than methane produced through the hydrogenotrophic pathway (i.e. CO_2 reduction). Whether or not the expression of clumped disequilibrium, and its extent, depends on metabolic pathways is still an active subject of research, which is beyond the scope of this study. Gruen et al. (2018) recently dedicated a series of experiments to explore the expression of $\Delta^{13}CH_3D$ disequilibrium among different methanogenic species and different metabolic pathways, including methylotrophic, hydrogenotrophic and acetoclastic pathways. While they suggest that part of the disequilibrium observed in the methylotrophic pathway may be inherited from the methyl precursor (Wang et al., 2015) (in other word, from the ^{13}C-D composition of the methanol substrate), overall their results tend to suggest that clumped disequilibrium may not depend on the metabolic pathway. According to Gruen et al. (2015), disequilibrium arises during enzymatic reactions that are common to all pathways (such as the last step of methyl-coenzyme M reduction), suggesting that the extent of disequilibrium is controlled at first order by the rate of methanogenesis (Wang et al., 2015, Stolper et al., 2015; Gruen, 2018). Overall, although we have not characterized the ^{13}C-D composition of the methanol substrate used for the cultures in this study, the dramatic $\Delta^{12}CH_2D_2$ depletions compared to $\Delta^{13}CH_3D$ depletions for both methylotrophic and hydrogenotrophic pathways, suggests that clumped disequilibrium may not be controlled entirely by classic kinetics, and may also result from quantum tunneling of hydrogen atoms as previously suggested by Young et al. (2017), or from combinatorial (statistical) effects of drawing hydrogen from multiple reservoirs (Yeung et al., 2016, Young et al., 2017).

From Fig. 5, it is remarkable that all Silurian gases (as well as two Devonian gases) deviate from the equilibrium curve in the 'clumped space' and plot in a similar region to methane from methanogenic cultures (here, from the CO_2-reduction pathway). These disequilibria are all associated with low $\delta^{13}C$ and δD compositions (Fig. 3a), which by themselves could be indicative of a microbial methanogenesis contribution (e.g. Whiticar et al., 1986; Etiope and Sherwood Lollar, 2013), or an early thermogenic generation (Schoell, 1988; Hunt, 1996; Etiope et al., 2009). Their wet gas contents (characterized by C_1/C_{2+} ratio ranging between ~1 and 10) are *a priori* more reflective of a thermogenic origin. It can be noted that for some of these samples, if only $\Delta^{13}CH_3D$ was measured, the inferred temperature would have been apparently reasonable with thermogenic formation temperatures (ranging between 101 °C and 200 °C – Table 3). Other samples with elevated $\Delta^{13}CH_3D$-based temperatures (> 270 °C) are not consistent with thermogenic temperatures (an evidence for disequilibrium according to Stolper et al., 2017).

Here the addition of the data for the abundance of a second clumped isotopologue, $\Delta^{12}CH_2D_2$, confirms the prevalence of disequilibrium for all of these natural gas samples. Because to date similarly large disequilibrium in both $\Delta^{13}CH_3D$ and $\Delta^{12}CH_2D_2$ has only been reported for laboratory cultures (this study, Young et al., 2017), one can question whether disequilibrium is necessary indicative of microbial methanogenesis or if it could result as well from thermogenic generation and/or processes related to gas migration (Stolper et al., 2017; Shuai et al., 2018). In what follows, we discuss why the observed Silurian disequilibrium trend reflects, to first order, a mixing between two different sources of methane, and why the disequilibrium endmember observed in these natural gases is likely of microbial origin (despite the apparent low C_1/C_{2+} ratios).

5.2.1. Mixing different sources of methane in the Silurian units

Silurian samples from Southwest Ontario display variable degrees of disequilibrium in the clumped space. This variability of $\Delta^{13}CH_3D$ and $\Delta^{12}CH_2D_2$ correlates with the variability observed in the $\delta^{13}C$-δD space (Fig. 3a and c). As noted previously, the broad correlation between $\delta^{13}C$ and δD has been interpreted to reflect various degrees of mixing between an isotopically enriched methane (mostly present in Cambrian and Ordovician units), and more depleted methane present in Silurian units (Sherwood Lollar et al., 1994). Here the addition of clumped isotopologues adds further support to this mixing scenario between two sources of methane: one, nearly equilibrated in the clumped space with higher $\delta^{13}C$ and δD values, and one exhibiting strong disequilibrium with lower $\delta^{13}C$ and δD values (see Fig. 6). Mixing between methane endmembers can yield non-linearity effects of $\Delta^{13}CH_3D$ and $\Delta^{12}CH_2D_2$ scaling (more broadly discussed by Eiler and Schauble, 2004 for CO_2 isotopologues). Young et al. (2016, 2017) have shown that mixing can result in significant departures from the equilibrium curve in $\Delta^{13}CH_3D$-$\Delta^{12}CH_2D_2$ space and, while these non-linearity effects can add some complexity in interpreting clumped isotopologue signatures, they can also be a powerful tool to quantitatively resolve mixing (Young et al., 2016; Douglas et al., 2016), provided that the end-members are known, or at least estimated. For the mixing models shown in Fig. 6, the thermogenic methane endmember was assumed to be similar to the thermogenic gases found in Cambrian or the Ordovician units. Given the small variability observed for these samples, both in terms of clumped (with equivalent temperatures ranging between ~100 and 200 °C) and bulk isotopic compositions, we define the thermogenic endmember by averaging the six samples from Cambrian and Ordovician, yielding $\delta^{13}C = -39.7‰$, $\delta D = -189‰$, and $\Delta^{13}CH_3D$ and $\Delta^{12}CH_2D_2$ appropriate for a temperature of 155 °C. Similarly, we derived the disequilibrium endmember by averaging $\Delta^{13}CH_3D$ and $\Delta^{12}CH_2D_2$, $\delta^{13}C$ and δD compositions of the two most disequilibrium Silurian gases: *Ram No.33* in Southwest Ontario, and *State Chester-F* in the Michigan Basin. As it will be discussed below, the methane samples in the Silurian units with the greatest departures from equilibrium are not necessarily the "pure" endmembers and could themselves represent mixtures with an even more depleted endmember. Overall, this two-endmember mixing model is a first-order approximation for explaining the methane variability in these Paleozoic sections. The selected end-members are for the purposes of demonstrating possible fit to a mixing model.

5.2.2. Early thermogenic or relic microbial methanogenesis in Silurian Strata?

While at least one source of methane in the Silurian strata is almost certainly of thermogenic origin and likely plotting near or on the equilibrium curve in the clumped space (similar to Cambrian and Ordovician gases), the origin of the disequilibrium endmember can be examined. To date, most thermogenic gases investigated have revealed $\Delta^{13}CH_3D$, or $\Delta^{13}CH_3D$ and $\Delta^{12}CH_2D_2$, in relative agreement with formation temperatures, suggesting that thermogenic gases are generally formed at or close to internal isotopic equilibrium (Stolper et al., 2014b, 2015, 2017; Wang et al., 2015; Douglas et al., 2016, 2017; Young et al., 2018). Notable exceptions were found in some oil-associated unconventional gas reservoirs (Stolper et al., 2017; Douglas et al., 2017), where $\Delta^{13}CH_3D$-based temperatures as high as 340 °C (i.e. not consistent with thermogenic origin, nor with oil stability) were seemingly reflecting a disequilibrium, although the absence of $\Delta^{12}CH_2D_2$ measurements prevents direct comparison to the dataset in this study. This led Stolper et al. (2017) to consider the possibility for thermogenic methane to not be at internal equilibrium, and instead to reflect kinetic effects associated with methane generation, or gas migration, or even in the case of these unconventional gas reservoirs, with the oil and gas recovery method used (e.g. hydraulic fracturing). It should be noted that the latter is not applicable to the Silurian gases given the conventional nature of these reservoirs (Barker and Pollock, 1984).

The disequilibrium exhibited in these Silurian gases is unlikely to result from gas migration. During gas migration, diffusion is sometimes considered as viable process for isotope fractionation because of the relative difference of diffusion coefficients between isotopologues. As lighter isotopologues theoretically diffuse faster, the gas at the migration front would be depleted in $\delta^{13}C$ and δD, while the residual gas would be enriched in $\delta^{13}C$ and δD (e.g. Prinzhofer and Pernaton, 1997; Zhang and Kroos, 2001). The magnitude of isotope fractionation will depend on whether methane diffuses as a gas or through liquid solvent (e.g., water). In all cases though, $\Delta^{13}CH_3D$ and $\Delta^{12}CH_2D_2$ should be anti-correlated with $\delta^{13}C$ and δD (Young et al., 2017); which is not observed in our data. Furthermore, in the $\Delta^{13}CH_3D$-$\Delta^{12}CH_2D_2$ space, a physical fractionation by molecular mass (such as diffusion) must produce a 1:1 slope since both axes reflect 18/16 mass ratios, thus providing a reliable test for molecular mass fractionation (Young et al., 2017). Supposing that the original gas was plotting on the equilibrium curve (similar to gases from the Cambrian and Ordovician units), it is not possible to produce such depleted $\Delta^{12}CH_2D_2$ endmember values by diffusion alone.

Recent pyrolysis experiments (Shuai et al., 2018) demonstrated that disequilibrium $\Delta^{13}CH_3D$ values can be pro-

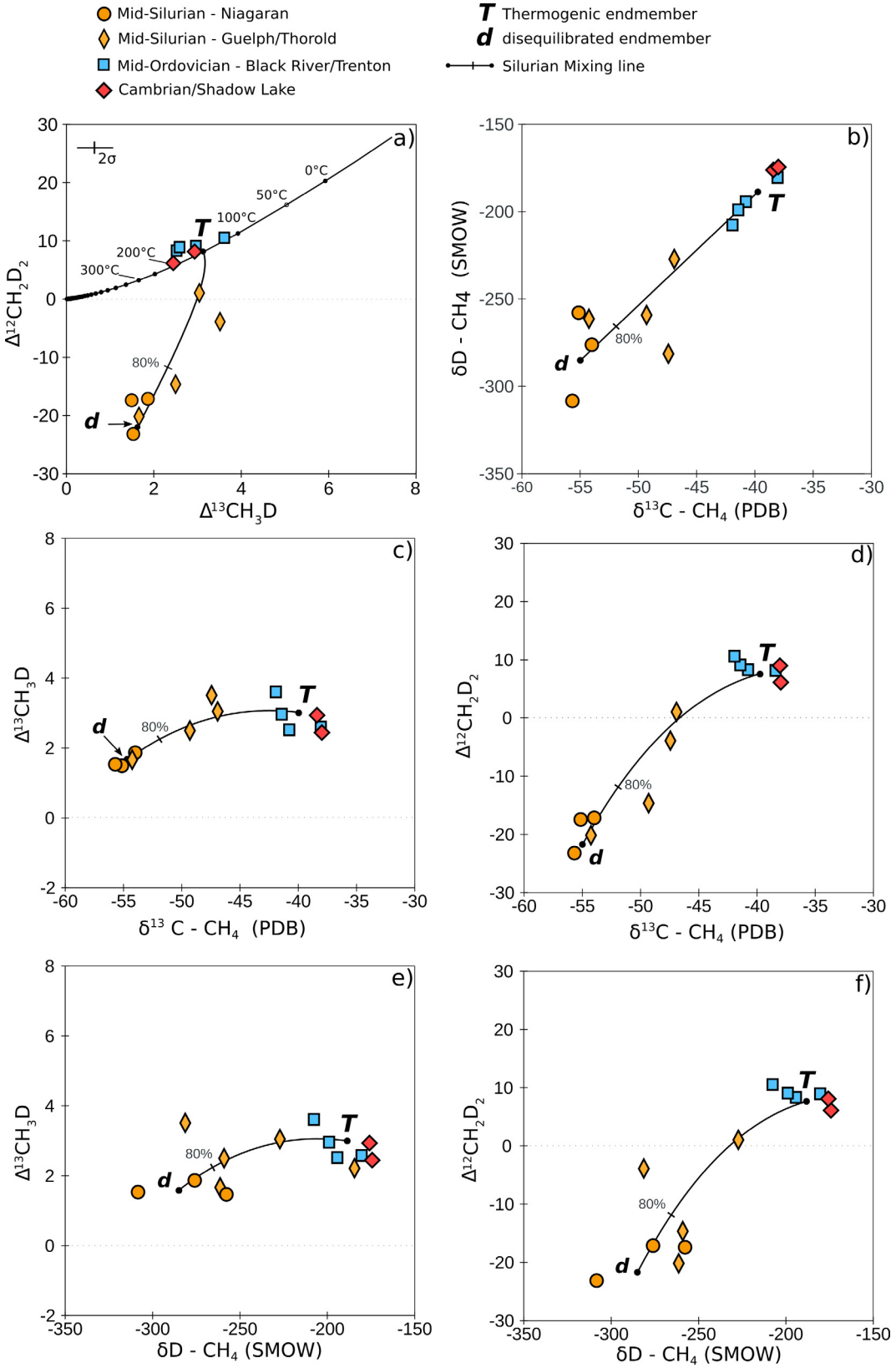

Fig. 6. First order mixing model between the mean of the most two most disequilibrated samples (d) and the mean of the most ^{13}C and D-enriched samples in Cambrian and Ordovician strata (assumed to be representative of the thermogenic endmember in the Silurian strata). All isotopic parameters are plotted versus each other, and demonstrate that both $\Delta^{13}CH_3D$-$\Delta^{12}CH_2D_2$ and $\delta^{13}C$-δD variations observed in the Silurian strata are best explained by a simple two-endmember mixing relationship.

duced at high thermal maturity (likely resulting from secondary cracking of wet gases particularly of ethane), but there is still paucity of experimental characterization of methane clumped compositions during thermogenic generation and cracking of different type of organic matter. In particular, it is not clear whether the large deficits in $\Delta^{12}CH_2D_2$ exhibited by microbial methanogenesis can also be produced during thermogenic generation. In the present case, it appears that a high-maturity scenario such as that explored by Shuai et al. (2018) is *a priori* not consistent with the low methane $\delta^{13}C$ and δD values measured in this study. Some would instead interpret the low $\delta^{13}C$ and δD values as indicative of an 'early' thermogenic generation (Schoell, 1988; Hunt, 1996; Etiope et al., 2009). The lack of experimental evidence for or against formation of similarly low $\Delta^{13}CH_3D$ and $\Delta^{12}CH_2D_2$ values by production of immature gases, means that we cannot formally exclude this as a possible explanation for the observed disequilibrium. However, in Silurian gases at least, the idea of significantly different maturity regime from Cambrian/Ordovician gases is not supported by the $\delta^{13}C$ and δD of ethane and propane that appear to be similar in range (Table 1 and Fig. 7) to the ethane and propane found in Cambrian and Ordovician formations (Barker and Pollock, 1984; Sherwood Lollar et al., 1994). This suggests relatively similar (if not identical) thermogenic gas components in terms of process and maturation levels for both Cambrian/Ordovician and Silurian gases (Sherwood Lollar et al., 1994).

Alternatively, based on existing data for $\Delta^{13}CH_3D$ as well as for $\Delta^{12}CH_2D_2$, the simplest explanation for the isotopic composition of the Silurian gases is that a microbial component mixing with the original thermogenic gas causes the low methane $\delta^{13}C$ and δD values and the strong disequilibrium observed in the clumped space. In Southwest Ontario, this hypothesis was first proposed by Sherwood Lollar et al. (1994) and was further supported by Clark et al. (2015), who explored the distribution of methane $\delta^{13}C$ and δD with depth. Importantly, the method they used (i.e. desorption from rock cores) not only allowed the measurement of $\delta^{13}C$ and δD with a fine depth resolution (approximately every ~ 5 m), but also allowed the measurement of $\delta^{13}C$ of CO_2 (which was systematically bellow detection limit in the present study). Clark et al. (2015) observed that gas samples with the lowest $\delta^{13}C$ and δD values (in their study, down to −53‰ and −330‰ respectively) were found in the thick Upper Ordovician black shale underlying the Silurian strata (see Fig. 1c), and were coinciding with sharp positive excursions of $\delta^{13}C$ of CO_2 (from −5‰ to +10‰) that are consistent with closed system microbial methanogenesis (e.g. Whiticar, 1999). According to this vertical profile therefore, the source for low methane $\delta^{13}C$ and δD in Silurian strata is likely originating from the underlying Upper Ordovician black shale (Clark et al., 2015). Overall, the low methane $\delta^{13}C$ and δD values, together with positive excursions of $\delta^{13}C$ of CO_2 (Clark et al., 2015), and large $\Delta^{13}CH_3D$ and $\Delta^{12}CH_2D_2$ deficits now provided by this study, are all strong arguments in favor of a microbial component of methane in the Silurian gases that are explored here.

Invoking microbial addition of methane despite low and rather homogeneous C_1/C_{2+} (from 1 to 10) might seem at first to be contradictory, because environments affected by microbial methanogenesis are generally expected to exhibit elevated $C_1/C_{2+} > 1000$. We note however, that elevated C_1/C_{2+} in sedimentary environments might reflect the combined effects of degradation of ethane and propane, in to net addition of methane (Martini et al., 2003, 2008). In fact, examination of mixing relationships between two sources of different C_1/C_{2+} ratios indicates that the resulting mixture is relatively insensitive to the elevated C_1/C_{2+} source. The mixture ratio (R) can be calculated as (Etiope and Sherwood Lollar, 2013)

$$1/R(f) = f/R_{\text{microbial}} + (1-f)/R_{\text{thermogenic}} \quad (7)$$

where f is the proportion of microbial methane added (typically $R_{\text{microbial}} = 10{,}000$). From Eq. (7) one finds that even 90% addition ($f = 0.9$) of microbial gas will only shift a low C_1/C_{2+} ratio of 1–10. In other words, a limited addition of microbial methane in Silurian gases could have significantly modified the bulk and the clumped isotopologue signatures of the mixture methane, while keeping the C_1/C_{2+} to rather low and seemingly thermogenic values. We note that the idea of a microbial methanogenesis contribution (associated with oil biodegradation, i.e. low thermal settings) was also proposed by Osborn and McIntosh (2010) and Etiope et al. (2013) for Devonian shales gases in the Appalachian Basin showing C_1/C_{2+} as low as 1.5 together with low bulk $\delta^{13}C$ and δD (−50 and −292‰, respectively). Using the concept of mixing to explain C_1/C_{2+}, and the $\delta^{13}C$-δD correlation (see Fig. 6b), a hypothetical microbial endmember with $\delta^{13}C = -65‰$ and $\delta D = -352‰$ can be inferred that reasonably satisfies C_1/C_{2+} ratios in Southwest Ontario Silurian gases, and suggests that they could contain as much as 60% microbially derived methane (Fig. 8a and b). This model requires a microbial endmember with a $\Delta^{13}CH_3D$ that is consistent with some of laboratory cultures (within 0.2‰ of *Methanosarcina barkeri* at 37 °C), but a $\Delta^{12}CH_2D_2$ significantly more depleted (>20‰) than existing laboratory culture data (Fig. 8c). Although this was not fully explored here (because of the lack of additional data), similar types of scenarios could be considered for the Dundee and the Berea samples, though they would require a thermogenic endmember with a lower C_1/C_{2+} (Fig. 8a).

Our understanding of large isotopologue disequilibrium effects, like those observed in these gas reservoirs, will benefit from further laboratory investigations on early thermogenic formation of methane. Nonetheless, based on the data to date, it appears that microbial methanogenesis is a likely explanation for the observed disequilibrium.

5.3. Low temperature microbial mediation in the Antrim Shale

In the Antrim Shale, microbial methanogenesis activity has been well documented, and proposed to be responsible for a substantial component of the methane found therein (Martini et al., 1996, 1998, 2003; Waldron et al., 2007; Kirk et al., 2012; Wuchter et al., 2013; Stolper et al.,

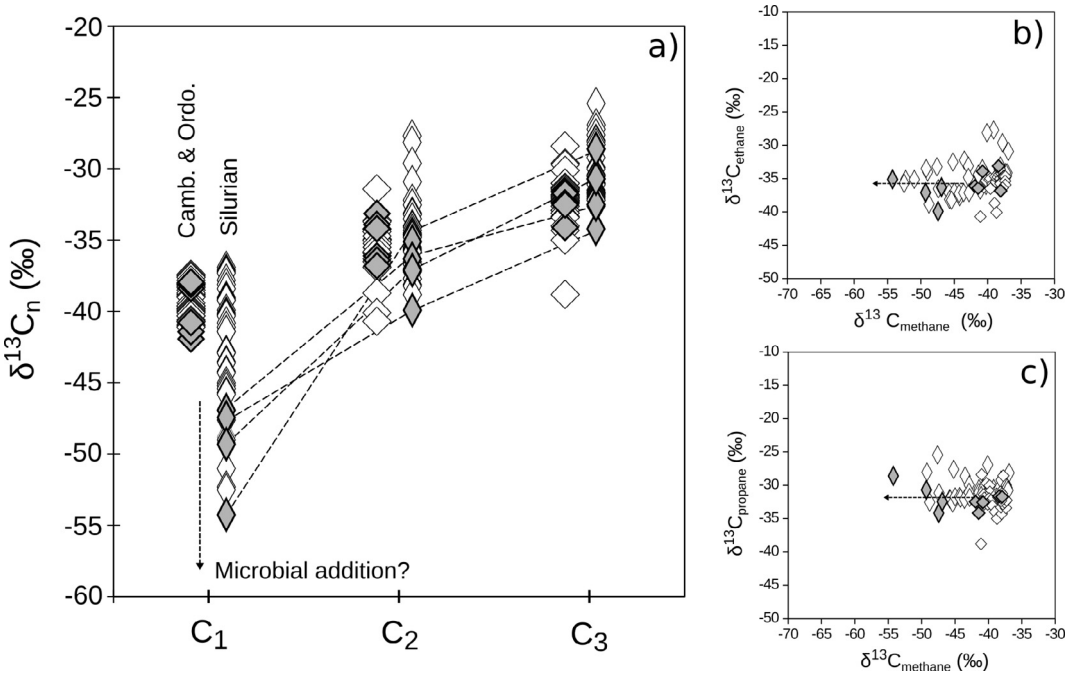

Fig. 7. Carbon stable isotope composition of methane (C_1), ethane (C_2) and propane (C_3) are reported for Cambrian & Ordovician units, and for Silurian units. Data in grey are samples measured in this study, data in white are from Barker and Pollock (1984) and Sherwood Lollar et al. (1994). Despite clear depletion of the methane $\delta^{13}C$ in the Silurian unit, $\delta^{13}C$ of ethane and propane appear in the same range that in Cambrian and Ordovician units, suggesting that thermogenic gas component(s) in all of these units are similar in terms of maturation levels.

2015). Here, this interpretation is apparently supported by the low methane $\delta^{13}C$ and δD values (Fig. 3a), as well as the relatively enriched $\delta^{13}C$ of CO_2 (12–17‰, Table 1), which is consistent with closed system methanogenesis (Martini et al., 1996; Whiticar, 1999; Stolper et al., 2015). The importance of Anaerobic Oxidation of Hydrocarbons (AOH) in the Antrim Shale has also been highlighted by Martini et al., (1998, 2003, 2008) and Budai et al. (2002). In particular, the biodegradation of ethane and propane, typically characterized by the systematic enrichment in ^{13}C (Pallasser et al., 2000) together with depletions of their relative concentrations, was proposed to be mostly responsible for the increase of C_1/C_{2+} values measured along the margins of the shale (Martini et al., 2003, 2008). In general, the degradation of methane (AOM) is thought to occur at lower rates than those for ethane or propane (Kniemeyer et al., 2007; Valentine et al., 2010; Adams et al., 2013; Bose et al., 2013; Meng et al., 2017). Despite evidence for methane being oxidized in incubated porewaters (Wuchter et al., 2013), the impact of AOM on Antrim Shale gases has been more difficult to assess, likely due to combined effects of methane microbial production (Martini et al., 1998, 2003). For instance, along the northern margin of the shale (Fig. 9; Stolper et al., 2015), the methane $\delta^{13}C$ and δD do not show typical enrichments expected for a system experiencing net methane depletion through AOM (Whiticar, 1999; Seifert et al., 2006; Holler et al., 2009). This contrasts with the western margin where small enrichments of the methane $\delta^{13}C$ (Martini et al., 2003) – also correlated to propane and ethane enrichments – could support the role of AOM in the formation (Fig. 9). According to Martini et al. (2003), the intensity of AOH in the Antrim Shale versus that of microbial methanogenesis must have been primarily controlled by the sulfate availability in the porewaters. While AOH is probably dominant after episodes of freshwater recharges (such as following Pleistocene glaciations) that are likely to add substantial amount of sulfate to the porewaters, microbial methanogenesis likely resumes as the dominant process once sulfate concentrations become sufficiently low. Currently, sulfate concentrations are extremely low in the Antrim Shale (<0.1 mM, Martini et al., 2003) which should therefore favor microbial methanogenesis (Kirk et al., 2012).

In this context, these samples from the Antrim Shale represent one of the first set of data with a significant microbial methane component that appear close to internal equilibrium ($\Delta^{13}CH_3D$ and $\Delta^{12}CH_2D_2$, Fig. 3c) and to external equilibrium (D/H fractionation between methane and water, Fig. 4). This observation was suggested by Stolper et al. (2015) who proposed that methane in the Antrim Shale reflected the mixing between two equilibrated endmembers, one of thermogenic origin (extrapolated to $T > 144$ °C, $C_1/C_{2+} \sim 6$) and one of microbial origin (extrapolated to $T \sim 20$ °C, $C_1/C_{2+} > 10{,}000$). Here, although our dataset does not cover the full range of C_1/C_{2+} variability explored by Stolper et al. (2015), the addition of $\Delta^{12}CH_2D_2$ data reinforces this idea of mixing between two nearly-equilibrated pools of methane. Though it should be noted the $\Delta^{13}CH_3D$ and $\Delta^{12}CH_2D_2$ measured in *North Charlton A1-18* (the most 'microbial' gas based

on C_1/C_{2+}) yield slightly different clumped-based temperatures (31 °C and 72 °C, respectively), suggesting slight disequilibrium is present in this endmember. In order to explain the apparent equilibrium of the microbial endmember (or the absence of kinetic effects typically observed in laboratory cultures), Stolper et al. (2015) developed a model based on the reasoning of Valentine et al. (2004) in which the degree of enzymatic reversibility during microbial methanogenesis controls the deviation from internal equilibrium with environmental temperatures. According to their model, the extremely slow formation rate under low H_2 availability results in nearly fully reversible methanogenesis in the Antrim Shale and in the formation of methane approaching both internal and external isotopic equilibrium (Stolper et al. 2015). While this interpretation might be valid, to date, attempts to observe the production of such near-equilibrium methane by methanogens in laboratory have been unsuccessful (Harder, 1997; Moran et al., 2005, 2007; Okumura et al., 2016). In other word, despite evidence for reversibility of one key enzyme involved in the methanogenesis pathway (Scheller et al., 2010), there

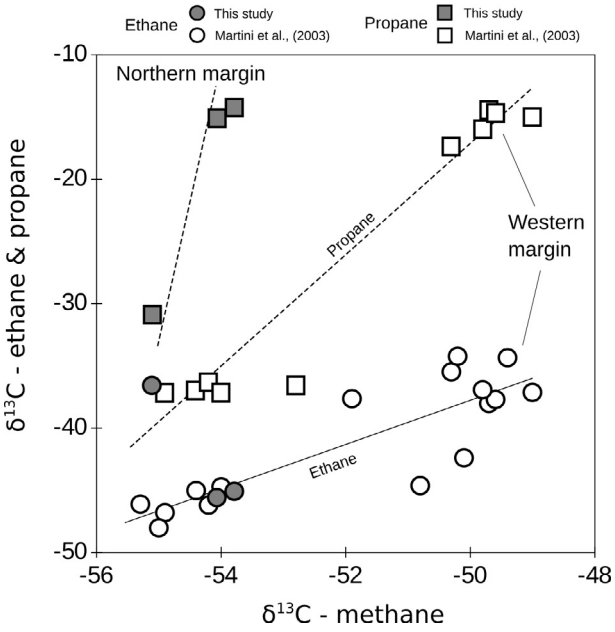

Fig. 9. Carbon stable isotope composition of ethane and propane in the Antrim Shale versus that of methane. Both in the Northern margin (this study) and in the Western margin (Martini et al., 2003), the $\delta^{13}C$ of ethane and propane tracks the significant influence of AOH in this sedimentary system (Martini et al., 1998, 2003). Remarkably, in the Western margin, the methane $\delta^{13}C$ also becomes progressively more enriched, possibly suggesting the role of AOM.

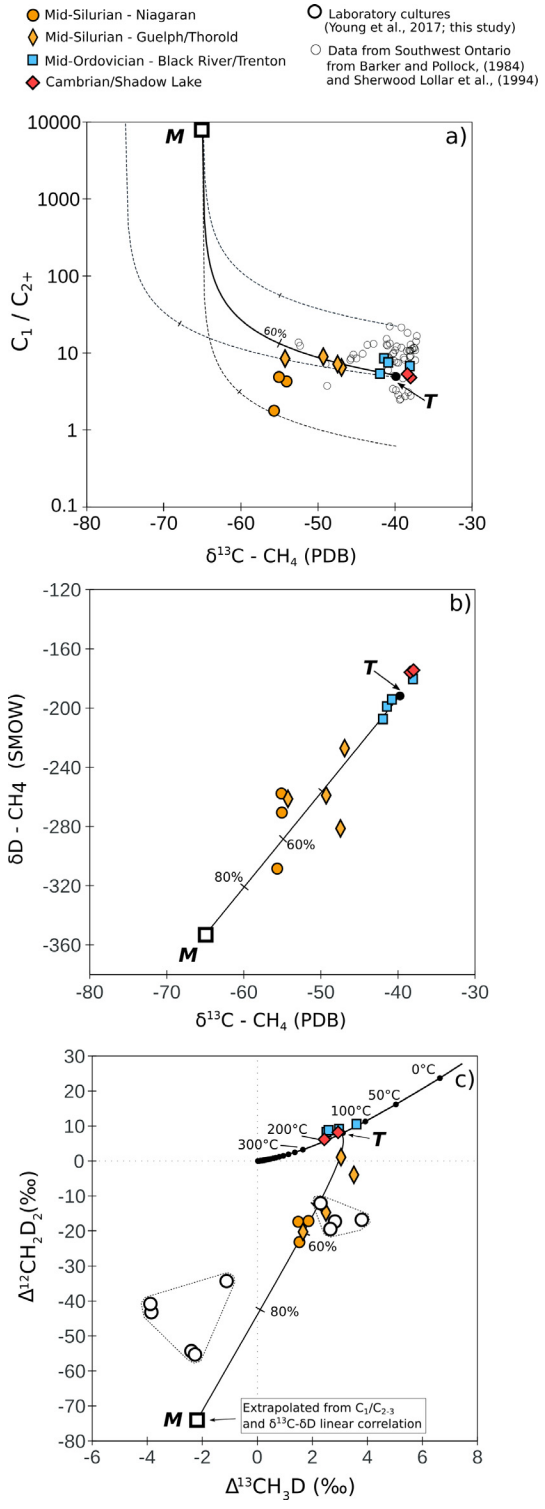

Fig. 8. Example of extrapolating a microbial endmember in the Silurian strata. Making the hypothesis that C_1/C_{2+} have not been altered by secondary processes, a maximum of 60–70% of microbially-derived methane could be present in the Silurian strata. (a) The $\delta^{13}C$ of the hypothetical endmember M can be extrapolated so that the mixing line (black line) fit the rather homogeneous C_1/C_{2+} observed in the Southwest Ontario data. Dashed-line indicate other potential mixing line using different thermogenic C_1/C_{2+} ratios, or a different $\delta^{13}C$ for the microbial endmember. (b) the δD of the microbial endmember is then extrapolated from linear mixing relationship between $\delta^{13}C$ and δD proposed in Fig. 6b. (c) $\Delta^{13}CH_3D$ and $\Delta^{12}CH_2D_2$ compositions are then extrapolated so that the resulting mixing line extends the mixing line between T and "d" reported in Fig. 6a.

is still no evidence that methanogens can act (nearly) fully reversibly; although this could be explained by the inability to reproduce geological conditions of growth in laboratory.

Here we suggest that near-equilibrium signature for the microbial endmember could also reflect the role of AOM (in addition to microbial methanogenesis). In natural environments, AOM is thought to mostly result from the syntrophic collaboration of methane oxidizing archaea and sulfate-reducing bacteria following: $CH_4 + SO_4^{2-}$ --> $HCO_3^- + HS^- + H_2O$ (e.g. Boetius et al., 2000). The relatively low standard-state Gibbs free energy of this reaction (<−35 kJ mol^{-1}, Shima and Thauer, 2005; Thauer, 2011) indicates that sulfate-dependent AOM can potentially operate at near thermodynamic equilibrium, with significant reversibility (Holler et al., 2011; Yoshinaga et al., 2014; Timmers et al., 2017; Marlow et al., 2017), although the actual free energies depend on the local chemistry of the environment. While under high sulfate concentrations the methane back-flux is 3–7% of the net AOM (Holler et al., 2011), it can reach up to 78% under extremely low sulfate concentrations (< 0.5 mM) (Yoshinaga et al., 2014). There is no published study so far on the effects of AOM on methane clumped isotopologues. Wang et al. (2016) investigated the kinetic isotope effects during aerobic oxidation by *Methylococcus capsulatus* and reported a progressive depletion of the $\Delta^{13}CH_3D$ together with enrichment of $\delta^{13}C$ and δD in the residual methane. As the ratio of isotope fractionation factors for $^{13}C/^{12}C$ and D/H was similar to the those measured under laboratory conditions for AOM (Holler et al., 2009), Wang et al. (2016) suggested that the kinetic effect on $^{13}CH_3D$ during AOM – which should not deviate too significantly from the product of $^{13}C/^{12}C$ and D/H fractionation factors – could be similar to that of aerobic oxidation. However, Wang et al. (2016) recognized these considerations are likely not applicable when sulfate content are low due to the potential effects of reversibility (i.e. significant methane back-flux during AOM). Indeed, Yoshinaga et al. (2014) observed that in conditions of high reversibility, such as in the sulfate-methane transition zone, the $^{13}C/^{12}C$ of the residual methane gradually re-equilibrates with the $^{13}C/^{12}C$ of the dissolved inorganic carbon (DIC), thus suggesting a microbial mediation towards thermodynamic equilibrium. Recently, Young et al. (2017) proposed that AOM could be similarly be involved in re-ordering methane bonds towards clumped isotopologue equilibrium in deep crystalline environments from the Witwatersand Basin (South Africa), where organisms performing AOM have been previously identified (based on molecular genetic analyses, Lau et al., 2016; Simkus et al., 2016). In the context of the Antrim Shale, the well-established role of AOH, together with the nearly equilibrated $\Delta^{13}CH_3D$ and $\Delta^{12}CH_2D_2$ signatures, comprise supporting evidence that AOM could be involved in re-ordering methane bonds towards isotopic equilibrium. Stolper et al. (2015) also mentioned this possibility, but they discarded it arguing that if AOM had an important role in the Antrim Shale, thermogenic gases should be re-equilibrated to low temperature as well. However, this reasoning may not to take into account the likelihood that microbial communities (including the one performing AOM) only colonized the shallowest part of the Antrim Shale (Fig. 10), along the margins, where the incursion of freshwaters favored their development (e.g. McIntosh et al., 2002). Ongoing laboratory experiments by several research groups are expected to provide the experimental data necessarily to resolve these various processes in the near future.

5.4. Implications for sources and sinks of methane in Southwest Ontario and Michigan Basin

5.4.1. Thermogenic gases in low maturity environments

Despite the apparent low thermal maturity of the Cambrian and Ordovician units in Southwest Ontario, our study confirms a predominantly thermogenic origin for these units. In particular, the good agreement between independent formation temperatures calculated from $\Delta^{13}CH_3D$ and $\Delta^{12}CH_2D_2$ (ranging from 110 to 204 °C) and fluid inclusion homogenization temperatures in dolomitic cements (Coniglio et al., 1994), suggests that the presence of thermogenic gases in these formations is related to the circulation of hydrothermal fluids responsible for the precipitation of dolomitic cements. The generation of these hydrothermal fluid must have been external to the Southwest Ontario Basin. For now, two possible scenarios are proposed to explain the source of these hydrothermal fluids: (i) hydrocarbon gases have been generated outside Southwest Ontario and have migrated in Cambrian and Ordovician formations together with hydrothermal fluids, or (ii) the incursion of hydrothermal fluids in Southwest Ontario have triggered, *in situ*, the generation of light hydrocarbons. It should be noted that several potential source rocks for oil generation have been proposed in the Ordovician Trenton formation by Powell et al. (1984) and Obermajer et al. (1998). Following the second scenario, those rocks could have been source rock for thermogenic gas generation as well.

5.4.2. Microbial generation and/or reprocessing of methane

Although microbial methanogenesis is recognized in a variety of geological and natural settings, its contribution to hydrocarbon reservoirs has been often investigated in sedimentary formations where the incursion of freshwaters, such as incursion events following Pleistocene glaciations, is evident (e.g. Martini et al., 1996, 1998, 2003; McIntosh et al., 2002,2004; Formolo et al., 2008; Vinson et al., 2017). In those systems, the presence and the activity of methanogens is attested to by a variety of microbiological and geochemical methods, from culturing and DNA isolations, to $^{13}C/^{12}C$ and D/H fractionations of methane with CO_2 and H_2O respectively (see review by Vinson et al., 2017). Importantly, these systems almost systematically indicate: (i) elevated C_1/C_{2+} which are seemingly consistent with microbial methanogenesis contribution (although Martini et al., 1998, 2003 highlighted the role of ethane and propane degradation in increasing C_1/C_{2+} ratios), and (ii) relatively dilute porewaters with depleted $\delta^{18}O$ and δD values indicative of meteoric and/or glacial meltwater addition. Taken together these correlated parameters suggest that dilution of saline brine by meteoric water and/or glacial meltwater recharge in these sedimentary

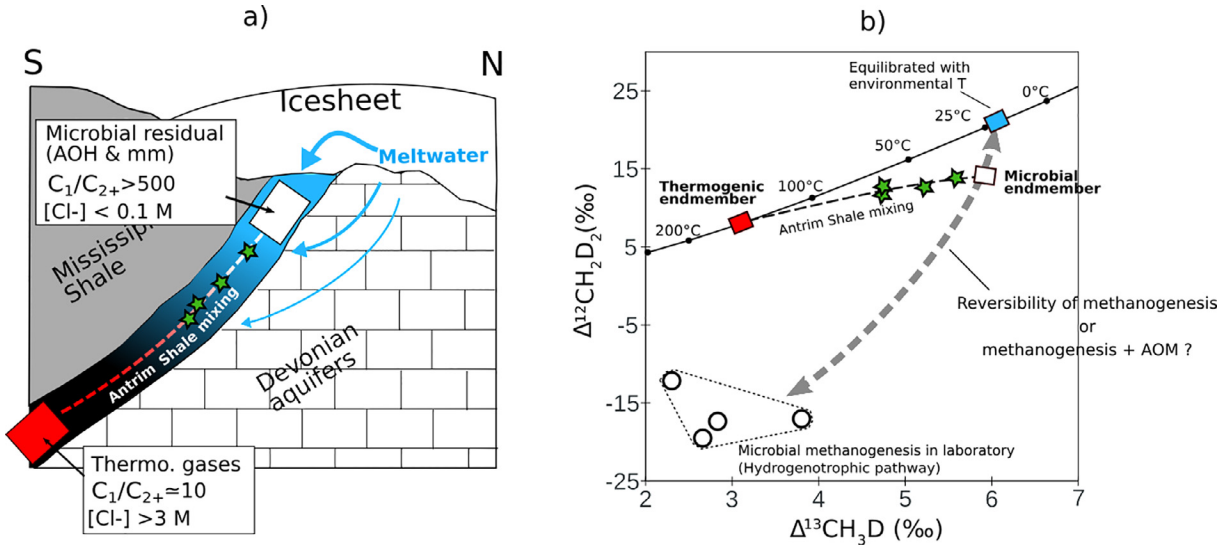

Fig. 10. Conceptual mixing scenario between thermogenic and microbial gases in the Antrim Shale. (a) Sketch of a South-to-North cross-section of the Antrim Shale and surrounding units. In the Antrim Shale, pristine thermogenic gases are present in more central and deeper part of the Michigan Basin, together with extremely saline brines ([Cl^-]> 3 M). Input of freshwaters following glacial advances and retreats have created a salinity gradient from surface to depth across the cross-section, allowing the development of microbial communities in the shallowest parts of the shale. The microbial endmember has an elevated C_1/C_{2+} which might mostly reflect the degradation of ethane and propane along the margins. (b) In the $\Delta^{13}CH_3D$-$\Delta^{12}CH_2D_2$ space, the four samples measured in this study can still be viewed as reflecting a mixing between a thermogenic source (here set to ~144 °C, following Stolper et al., 2015) and a nearly-equilibrated microbial endmember. This microbial endmember is either solely deriving from methanogenesis with high reversibility (as proposed by Stolper et al., 2015), or could be resulting from the combine (or successive) effects of microbial methanogenesis and AOM.

basins triggered microbial methanogenesis by lowering salinity, and providing substrates such as DIC or acetate. Conventionally the Antrim Shale would typically be considered a case-study for microbial methanogenesis in subsurface continental sedimentary system. As highlighted by this work, measurements of $\Delta^{13}CH_3D$ and $\Delta^{12}CH_2D_2$ indicate that the microbial methane present in this formation is near thermodynamic equilibrium. This contrasts with the expression of extensive kinetic effects observed in methane derived from laboratory methanogen cultures (Stolper et al., 2015; Wang et al., 2015; Young et al., 2017; Gruen et al., 2018; this study).

In contrast, in Silurian strata from Southwest Ontario where microbial methanogenesis has also been proposed to contribute significantly to the methane pool (despite the high salinity and relatively low C_1/C_{2+} (Sherwood Lollar et al., 1994; Clark et al., 2015)). The measurement of $\Delta^{13}CH_3D$ and $\Delta^{12}CH_2D_2$ indicate clear disequilibrium of the methane. Although it is possible that as of yet unidentified kinetic effects during thermogenic generation may have had a role in promoting disequilibrium, if these disequilibrium signatures are indeed inherited from microbial methanogenesis, they would greatly contrast with the nearly equilibrated methane observed in the Antrim Shale. According to Stolper et al. (2015) and Wang et al. (2015), the expression of different degree of disequilibrium could reflect different rates of microbial methanogenesis, resulting from variable substrate availability in sedimentary formations. Alternatively, here we suggest that nearly equilibrated methane could reflect the additional effect of AOM, which has been demonstrated to be associated with high degree of reversibility (Holler et al., 2011; Yoshinaga et al., 2014) that can result in $^{13}C/^{12}C$ re-equilibration of the residual methane under low sulfate conditions (Yoshinaga et al., 2014). The idea that AOM could have an impact on the methane pool in the Antrim Shale appears relevant, given the consistent role of anaerobic oxidation of hydrocarbons such as ethane and propane in this particular formation (Martini et al., 1998, 2003). Additional controlled laboratory investigations are needed to demonstrate that AOM, particularly in low sulfate conditions, would contribute to re-equilibration of both $\Delta^{13}CH_3D$ and $\Delta^{12}CH_2D_2$.

6. CONCLUSIONS

Depending on the processes involved, the methane cycle involves processes controlled by either at thermodynamic equilibrium effects or with large kinetic effects. Therefore, being able to determine whether methane is at thermodynamic equilibrium or not, is key to understanding and identifying subsurface methane sources and sinks. While the measurement of $\Delta^{13}CH_3D$ alone may provide relevant information on isotope bond ordering, independent estimates of environmental temperatures are required to confirm thermodynamic equilibrium (Stolper et al., 2014, 2015; Wang et al., 2015). This study demonstrates that the measurement of $\Delta^{12}CH_2D_2$, when combined with $\Delta^{13}CH_3D$, offers a sensitive indicator of the degree to which methane is at thermodynamic equilibrium or where its fate is controlled by disequilibrium (kinetic) processes. Accord-

ingly, $\Delta^{13}CH_3D$ and $\Delta^{12}CH_2D_2$ can only be interpreted in terms of formation temperature of methane when the two reflect the same apparent formation temperature, as this provides proof of consistency with internal thermodynamic equilibrium. In instances where apparent temperatures do not agree and methane isotopologues do not reflect internal equilibrium however, $\Delta^{13}CH_3D$ and $\Delta^{12}CH_2D_2$ can be used to interpret and identify methane cycling dominated by the expression of kinetic isotope effects (Young et al., 2017). The main conclusions of this study demonstrated that:

(1) The investigation of $\Delta^{12}CH_2D_2$ (combined with $\Delta^{13}CH_3D$) in gases from Cambrian and Ordovician strata, confirm the prevalence of thermodynamic equilibrium for these gases that are interpreted to derive from a thermogenic origin (Stolper et al., 2014, 2015; Wang et al., 2015; Young et al., 2017).
(2) In gas samples from the Silurian strata, the addition of $\Delta^{12}CH_2D_2$ measurements highlight the importance of identifying disequilibrium. Clumped disequilibrium is consistently associated with low bulk $\delta^{13}C$ and δD. While the effects of early thermogenic generation on clumped isotopologues remain to be explore, ethane and propane $\delta^{13}C$ support a maturity similar in Silurian and in Cambrian/Ordovician gases. Overall, the depletions observed in all four less abundant isotopologues ($^{13}CH_4$, $^{12}CH_3D$, $^{13}CH_3D$ and $^{12}CH_2D_2$), relative to Cambrian and Ordovician thermogenic gases, appear to be consistent with laboratory culture experiments for microbial methanogenesis and could support the presence of microbially-derived methane in these formations as suggested by previous authors (Sherwood Lollar et al., 1994; Clark et al., 2015).
(3) The quantitative evaluation of internal equilibrium permitted by the measurement of $\Delta^{13}CH_3D$ and $\Delta^{12}CH_2D_2$ has reinforced the idea, originally proposed by Stolper et al. (2015), that the microbial endmember associated with elevated C_1/C_{2+} in the Antrim Shale was approaching both internal and external equilibrium. While this observation could be explained by a high reversibility during low rate microbial methanogenesis (Stolper et al., 2015), we suggest this could well reflect the combined role of Anaerobic Oxidation of Methane (AOM), a process that typically operates near thermodynamic equilibrium (Timmers et al., 2017) and could re-process methane bonds towards clumped equilibrium (Yoshinaga et al., 2014; Young et al., 2017).

ACKNOWLEDGMENT

This study was supported by funding from the Natural Sciences and Engineering Research Council of Canada, the Sloan Foundation Deep Carbon Observatory and the Nuclear Waste Management Organization. The authors wish to thank Dr. Andrew Steele and Dr. Kosala Sirisena at the Carnegie Institution for helping culturing the Methanosarcina barkeri. The authors also wish to thank various industrial partners for their effort and support during sampling.

REFERENCES

Adams M. M., Hoarfrost A. L., Bose A., Joye S. B. and Girguis P. R. (2013) Anaerobic oxidation of short-chain alkanes in hydrothermal sediments: potential influences on sulfur cycling and microbial diversity. *Front. Microbiol.* **4**, 100.

Affek H. P., Xu X. and Eiler J. M. (2007) Seasonal and diurnal variations of $^{13}C^{18}O^{16}O$ in air: initial observations from Pasadena, CA. *Geochimica et Cosmochimica Acta* **71**(21), 5033–5043.

Al T. A., Clark I. D., Kennell L., Jensen M. and Raven K. G. (2015) Geochemical evolution and residence time of porewater in low-permeability rocks of the Michigan Basin, Southwest Ontario. *Chem. Geol.* **404**, 1–17.

Armstrong, D. K., & Carter, T. R. (2006). An updated guide to the subsurface Paleozoic stratigraphy of southern Ontario. Ontario Geological Survey.

Balch W. E., Fox G. E., Magrum L. J., Woese C. R. and Wolfe R. S. (1979) Methanogens: reevaluation of a unique biological group. *Microbiol. Rev.* **43**, 260–296.

Barker J. F. and Pollock S. J. (1984) The geochemistry and origin of natural gases in southern Ontario. *Bull. Can. Pet. Geol.* **32**(3), 313–326.

Bernard B. B., Brooks J. M. and Sackett W. M. (1976) Natural gas seepage in the Gulf of Mexico. *Earth Planet. Sci. Lett.* **31**(1), 48–54.

Brigham. R.J. 1971. Structural geology of Southwestern Ontario and southeastern Michigan. Ontario Dept. of Mines and Northern Affairs, Petroleum Resources Section, Paper 7 1-2, 110 p.

Boetius A., Ravenschlag K., Schubert C. J., Rickert D., Widdel F., Gieseke A. and Pfannkuche O. (2000) A marine microbial consortium apparently mediating anaerobic oxidation of methane. *Nature* **407**(6804), 623–626.

Bose A., Rogers D. R., Adams M. M., Joye S. B. and Girguis P. R. (2013) Geomicrobiological linkages between short-chain alkane consumption and sulfate reduction rates in seep sediments. *Front. Microbiol.*, 4.

Budai J. M., Martini A. M., Walter L. M. and Ku T. C. W. (2002) Fracture-fill calcite as a record of microbial methanogenesis and fluid migration: a case study from the Devonian Antrim Shale Michigan Basin. *Geofluids* **2**(3), 163–183.

Carter T. R., Trevail R. A. and Easton R. M. (1996) Basement controls on some hydrocarbon traps in southern Ontario Canada. *Special Papers-Geol. Soc. Am.*, 95–108.

Clark I. D., Al T., Jensen M., Kennell L., Mazurek M., Mohapatra R. and Raven K. G. (2013) Paleozoic-aged brine and authigenic helium preserved in an Ordovician shale aquiclude. *Geology* **41** (9), 951–954.

Clark I. D., Ilin D., Jackson R. E., Jensen M., Kennell L., Mohammadzadeh H. and Raven K. G. (2015) Paleozoic-aged microbial methane in an Ordovician shale and carbonate aquiclude of the Michigan Basin, southwestern Ontario. *Org. Geochem.* **83**, 118–126.

Clayton C. (1991) Carbon isotope fractionation during natural gas generation from kerogen. *Mar. Pet. Geol.* **8**(2), 232–240.

Coniglio, M., Sherlock, R., Williams-Jones, A. E., Middleton, K. and Frape, S. K. (1994) Burial and hydrothermal diagenesis of Ordovician carbonates from the Michigan Basin, Ontario, Canada. Dolomites—A volume in honour of Dolomieu. (eds. B. Purser, M. Tucker and D. Zenger). International Association of Sedimentologists, Special Publication, 21, 231–254.

Davies G. R. and Smith, Jr, L. B. (2006) Structurally controlled hydrothermal dolomite reservoir facies: an overview. *AAPG Bull.* **90**(11), 1641–1690.

Dollar, P. S., Frape, S. K., & McNuff, R. H. (1991). Geochemistry of formation waters, southwestern Ontario, Canada and southern Michigan, USA: Implications for origin and evolution. Queen's Printer for Ontario.

Dorr J. A. and Eschman D. F. (1970) *Geology of Michigan*. University of Michigan Press.

Douglas P. M. J., Stolper D. A., Smith D. A., Anthony K. W., Paull C. K., Dallimore S. and Sessions A. L. (2016) Diverse origins of Arctic and Subarctic methane point source emissions identified with multiply-substituted isotopologues. *Geochim. Cosmochim. Acta* **188**, 163–188.

Douglas P. M., Stolper D. A., Eiler J. M., Sessions A. L., Lawson M., Shuai Y. and Niemann M. (2017) Methane clumped isotopes: progress and potential for a new isotopic tracer. *Org. Geochem.*.

Eiler J. M. and Schauble E. (2004) $^{18}O^{13}C^{16}O$ in Earth's atmosphere. *Geochim. Cosmochim. Acta* **68**(23), 4767–4777.

Eiler J. M. (2007) "Clumped-isotope" geochemistry—the study of naturally-occurring, multiply-substituted isotopologues. *Earth Planet. Sci. Lett.* **262**(3–4), 309–327.

Etiope G. and Sherwood Lollar B. (2013) Abiotic methane on Earth. *Rev. Geophys.* **51**(2), 276–299.

Etiope G., Feyzullayev A., Milkov A. V., Waseda A., Mizobe K. C. H. S. and Sun C. H. (2009) Evidence of subsurface anaerobic biodegradation of hydrocarbons and potential secondary methanogenesis in terrestrial mud volcanoes. *Mar. Pet. Geol.* **26**(9), 1692–1703.

Etiope G., Drobniak A. and Schimmelmann A. (2013) Natural seepage of shale gas and the origin of "eternal flames" in the Northern Appalachian Basin, USA. *Mar. Pet. Geol.* **43**, 178–186.

Ferry J. M., Passey B. H., Vasconcelos C. and Eiler J. M. (2011) Formation of dolomite at 40–80 C in the Latemar carbonate buildup, Dolomites, Italy, from clumped isotope thermometry. *Geology* **39**(6), 571–574.

Formolo M. J., Salacup J. M., Petsch S. T., Martini A. M. and Nusslein K. (2008) A new model linking atmospheric methane sources to Pleistocene glaciation via methanogenesis in sedimentary basins. *Geology* **36**(2), 139–142.

Ghosh P., Adkins J., Affek H., Balta B., Guo W., Schauble E. A. and Eiler J. M. (2006) ^{13}C–^{18}O bonds in carbonate minerals: a new kind of paleothermometer. *Geochim. Cosmochim. Acta* **70**(6), 1439–1456.

Gruen D. S., Wang D. T., Könneke M., Topçuoğlu B. D., Stewart L. C., Goldhammer T. and Ono S. (2018) Experimental investigation on the controls of clumped isotopologue and hydrogen isotope ratios in microbial methane. *Geochim. Cosmochim. Acta*.

Gutschick R. C. and Sandberg C. A. (1991) Late Devonian history of Michigan basin. *Geol. Soc. Am. Spec. Pap.* **256**, 181–202.

Haeri-Ardakani O., Al-Aasm I. and Coniglio M. (2013) Fracture mineralization and fluid flow evolution: an example from Ordovician-Devonian carbonates, southwestern Ontario, Canada. *Geofluids* **13**(1), 1–20.

Harder J. (1997) Anaerobic methane oxidation by bacteria employing 14C-methane uncontaminated with 14C-carbon monoxide. *Mar. Geol.* **137**(1–2), 13–23.

Hobbs M. Y., Frape S. K., Shouakar-Stash O. and Kennell L. R. (2011) Regional Hydrogeochemistry-Southern Ontario. *Nuclear Waste Management Organization Report*, 157.

Holler T., Wegener G., Knittel K., Boetius A., Brunner B., Kuypers M. M. and Widdel F. (2009) Substantial $^{13}C/^{12}C$ and D/H fractionation during anaerobic oxidation of methane by marine consortia enriched in vitro. *Environ. Microbiol. Rep.* **1**(5), 370–376.

Holler T., Wegener G., Niemann H., Deusner C., Ferdelman T. G., Boetius A. and Widdel F. (2011) Carbon and sulfur back flux during anaerobic microbial oxidation of methane and coupled sulfate reduction. *Proc. Natl. Acad. Sci.* **108**(52), E1484–E1490.

Horibe Y. and Craig H. (1995) DH fractionation in the system methane-hydrogen-water. *Geochimica et Cosmochimica Acta* **59**(24), 5209–5217.

Horita J. and Wesolowski D. J. (1994) Liquid-vapor fractionation of oxygen and hydrogen isotopes of water from the freezing to the critical temperature. *Geochimica et Cosmochimica Acta* **58**(16), 3425–3437.

Horita J. and Berndt M. E. (1999) Abiogenic methane formation and isotopic fractionation under hydrothermal conditions. *Science* **285**(5430), 1055–1057.

Hunt J. M. (1996). *Petroleum geochemistry and geology* **Vol. 2**, 1–743.

Ijiri A., Inagaki F., Kubo Y., Adhikari R. R., Hattori S., Hoshino T. and Ono S. (2018) Deep-biosphere methane production stimulated by geofluids in the Nankai accretionary complex. *Sci. Adv.* **4**(6), eaao4631.

Inagaki F., Hinrichs K. U., Kubo Y., Bowles M. W., Heuer V. B., Hong W. L. and Kaneko M. (2015) Exploring deep microbial life in coal-bearing sediment down to~ 2.5 km below the ocean floor. *Science* **349**(6246), 420–424.

James A. T. (1983) Correlation of natural gas by use of carbon isotopic distribution between hydrocarbon components. *AAPG Bull.* **67**(7), 1176–1191.

Johnson M. D., Armstrong D. K., Sanford B. V., Telford P. G. and Rutka M. A. (1992) Paleozoic and Mesozoic geology of Ontario. *Geology of Ontario, Ontario Geological Survey Special* **4**, 907–1008.

Jones W. J., Paynter M. J. B. and Gupta R. (1983) Characterization of Methanococcus maripaludis sp. nov., a new methanogen isolated from salt marsh sediment. *Arch. Microbiol.* **135**(2), 91–97.

Kendall M. M., Liu Y., Sieprawska-Lupa M., Stetter K. O., Whitman W. B. and Boone D. R. (2006) Methanococcus aeolicus sp. nov., a mesophilic, methanogenic archaeon from shallow and deep marine sediments. *IJSEM* **56**, 1525–1529.

Kharaka Y. K. and Hanor J. S. (2003) Deep fluids in the continents: I Sedimentary basins. *Treatise Geochem.* **5**, 605.

Kirk M. F., Martini A. M., Breecker D. O., Colman D. R., Takacs-Vesbach C. and Petsch S. T. (2012) Impact of commercial natural gas production on geochemistry and microbiology in a shale-gas reservoir. *Chem. Geol.* **332**, 15–25.

Knauth L. P. and Beeunas M. A. (1986) Isotope geochemistry of fluid inclusions in Permian halite with implications for the isotopic history of ocean water and the origin of saline formation waters. *Geochim. Cosmochim. Acta* **50**(3), 419–433.

Kniemeyer O., Musat F., Sievert S. M., Knittel K., Wilkes H., Blumenberg M. and Widdel F. (2007) Anaerobic oxidation of short-chain hydrocarbons by marine sulphate-reducing bacteria. *Nature* **449**(7164), 898–901.

Knittel K. and Boetius A. (2009) Anaerobic oxidation of methane: progress with an unknown process. *Annu. Rev. Microbiol.* **63**, 311–334.

Lau M. C., Kieft T. L., Kuloyo O., Linage-Alvarez B., Van Heerden E., Lindsay M. R. and Perlman D. H. (2016) An oligotrophic deep-subsurface community dependent on syntrophy is dominated by sulfur-driven autotrophic denitrifiers. *Proc. Natl. Acad. Sci.*, 201612244.

Legall F. D., Barnes C. R. and Macqueen R. W. (1981) Thermal maturation, burial history and hotspot development, Paleozoic strata of southern Ontario-Quebec, from conodont and acritarch colour alteration studies. *Bull. Can. Pet. Geol.* **29**(4), 492–539.

Liu Q. and Liu Y. (2016) Clumped-isotope signatures at equilibrium of CH_4, NH_3, H_2O, H_2S and SO_2. *Geochim. Cosmochim. Acta* **175**, 252–270.

Lorant F., Prinzhofer A., Behar F. and Huc A. Y. (1998) Carbon isotopic and molecular constraints on the formation and the expulsion of thermogenic hydrocarbon gases. *Chem. Geol.* **147** (3–4), 249–264.

Ma L., Castro M. C., Hall C. M. and Walter L. M. (2005) Cross-formational flow and salinity sources inferred from a combined study of helium concentrations, isotopic ratios, and major elements in the Marshall aquifer, southern Michigan. *Geochem. Geophys. Geosyst.* **6**(10).

Ma Q., Wu S. and Tang Y. (2008) Formation and abundance of doubly-substituted methane isotopologues (13CH3D) in natural gas systems. *Geochim. Cosmochim. Acta* **72**(22), 5446–5456.

Marlow J. J., Steele J. A., Ziebis W., Scheller S., Case D., Reynard L. M. and Orphan V. J. (2017) Monodeuterated methane, an isotopic tool to assess biological methane metabolism rates. *mSphere* **2**(4), e00309-17.

Martini, A. M., Budai, J. M., Walter, L. M. and Schoell, M. (1996) Microbial generation of economic accumulations of methane within a shallow organic-rich shale.

Martini A. M., Walter L. M., Budai J. M., Ku T. C. W., Kaiser C. J. and Schoell M. (1998) Genetic and temporal relations between formation waters and biogenic methane: Upper Devonian Antrim Shale, Michigan Basin, USA. *Geochimica et Cosmochimica Acta* **62**(10), 1699–1720.

Martini A. M., Walter L. M., Ku T. C., Budai J. M., McIntosh J. C. and Schoell M. (2003) Microbial production and modification of gases in sedimentary basins: a geochemical case study from a Devonian shale gas play, Michigan basin. *AAPG Bulletin* **87**(8), 1355–1375.

Martini A. M., Walter L. M. and McIntosh J. C. (2008) Identification of microbial and thermogenic gas components from Upper Devonian black shale cores Illinois and Michigan basins. *Aapg Bulletin* **92**(3), 327–339.

Mazurek M. (2004) Long-term used nuclear fuel waste management: geoscientific review of the sedimentary sequence in Southern Ontario. *Nucl. Waste Manage. Organization*.

McIntosh J. C. and Walter L. M. (2005) Volumetrically significant recharge of Pleistocene glacial meltwaters into epicratonic basins: constraints imposed by solute mass balances. *Chem. Geol.* **222**(3), 292–309.

McIntosh J. C., Walter L. M. and Martini A. M. (2004) Extensive microbial modification of formation water geochemistry: case study from a Midcontinent sedimentary basin, United States. *Geol. Soc. Am. Bull.* **116**(5–6), 743–759.

McIntosh J. C., Garven G. and Hanor J. S. (2011) Impacts of Pleistocene glaciation on large-scale groundwater flow and salinity in the Michigan Basin. *Geofluids* **11**(1), 18–33.

McIntosh J. C., Schlegel M. E. and Person M. (2012) Glacial impacts on hydrologic processes in sedimentary basins: evidence from natural tracer studies. *Geofluids* **12**(1), 7–21.

McIntosh J. C., Walter L. M. and Martini A. M. (2002) Pleistocene recharge to midcontinent basins: effects on salinity structure and microbial gas generation. *Geochim. Cosmochim. Acta* **66** (10), 1681–1700.

Meng Q., Wang X., Wang X., Shi B., Luo X., Zhang L. and Liu P. (2017) Gas geochemical evidences for biodegradation of shale gases in the Upper Triassic Yanchang Formation, Ordos Basin, China. *Int. J. Coal Geol.* **179**, 139–152.

Moran J. J., House C. H., Freeman K. H. and Ferry J. G. (2005) Trace methane oxidation studied in several Euryarchaeota under diverse conditions. *Archaea* **1**(5), 303–309.

Moran J. J., House C. H., Thomas B. and Freeman K. H. (2007) Products of trace methane oxidation during nonmethyltrophic growth by Methanosarcina. *J. Geophys. Res. Biogeosci.* **112** (G2).

Obermajer M., Fowler M. G., Goodarzi F. and Snowdon L. R. (1996) Assessing thermal maturity of Palaeozoic rocks from reflectance of chitinozoa as constrained by geochemical indicators: an example from southern Ontario Canada. *Marine and Petroleum Geology* **13**(8), 907–919.

Obermajer M., Fowler M. G. and Snowdon L. R. (1998) A geochemical characterization and a biomarker re-appraisal of the oil families from southwestern Ontario, Canada. *Bull. Can. Petrol. Geol.* **46**(3), 350–378.

Okumura T., Kawagucci S., Saito Y., Matsui Y., Takai K. and Imachi H. (2016) Hydrogen and carbon isotope systematics in hydrogenotrophic methanogenesis under H 2-limited and H 2-enriched conditions: implications for the origin of methane and its isotopic diagnosis. *Prog. Earth Planet. Sci.* **3**(1), 14.

Ono S., Wang D. T., Gruen D. S., Sherwood Lollar B., Zahniser M. S., McManus B. J. and Nelson D. D. (2014) Measurement of a doubly substituted methane isotopologue, 13CH3D, by tunable infrared laser direct absorption spectroscopy. *Anal. Chem.* **86**(13), 6487–6494.

Oren A. (2011) Thermodynamic limits to microbial life at high salt concentrations. *Environ. Microbiol.* **13**(8), 1908–1923.

Osborn S. G. and McIntosh J. C. (2010) Chemical and isotopic tracers of the contribution of microbial gas in Devonian organic-rich shales and reservoir sandstones, northern Appalachian Basin. *Appl. Geochem.* **25**(3), 456–471.

Pallasser R. J. (2000) Recognising biodegradation in gas/oil accumulations through the $\delta^{13}C$ compositions of gas components. *Org Geochem.* **31**(12), 1363–1373.

Powell T. G., Macqueen R. W., Barker J. F. and Bree D. G. (1984) Geochemical character and origin of Ontario oils. *Bull. Can. Pet. Geol.* **32**(3), 289–312.

Prinzhofer A. and Pernaton E. (1997) Isotopically light methane in natural gas: bacterial imprint or diffusive fractionation? *Chem. Geol.* **142**(3–4), 193–200.

Sanford B. V., Thompson F. J. and McFall G. H. (1985) Plate tectonics–a possible controlling mechanism in the development of hydrocarbon traps in southwestern Ontario. *Bull. Can. Pet. Geol.* **33**(1), 52–71.

Sanford B. V. (1993) St. Lawrence Platform - Geology. In *Sedimentary cover of the craton in Canada. Geological Survey Canada* (eds. D. F. Stott and J. D. Aitken). Geology of Canada, pp. 723–786.

Schoell M. (1988) Multiple origins of methane in the Earth. *Chem. Geol.* **71**(1–3), 1–10.

Scheller S., Goenrich M., Boecher R., Thauer R. K. and Jaun B. (2010) The key nickel enzyme of methanogenesis catalyses the anaerobic oxidation of methane. *Nature* **465**(7298), 606.

Seifert R., Nauhaus K., Blumenberg M., Krüger M. and Michaelis W. (2006) Methane dynamics in a microbial community of the Black Sea traced by stable carbon isotopes in vitro. *Org Geochem.* **37**(10), 1411–1419.

Sherwood Lollar B., Frape S. K., Weise S. M., Fritz P., Macko S. A. and Welhan J. A. (1993) Abiogenic methanogenesis in crystalline rocks. *Geochim. Cosmochim. Acta* **57**(23–24), 5087–5097.

Sherwood Lollar B., Weise S. M., Frape S. K. and Barker J. F. (1994) Isotopic constraints on the migration of hydrocarbon and helium gases of southwestern Ontario. *Bull. Can. Pet. Geol.* **42**(3), 283–295.

Sherwood Lollar B., Westgate T. D., Ward J. A., Slater G. F. and Lacrampe-Couloume G. (2002) Abiogenic formation of alkanes in the Earth's crust as a minor source for global hydrocarbon reservoirs. *Nature* **416**(6880), 522–524.

Sherwood Lollar B. and Ballentine C. J. (2009) Insights into deep carbon derived from noble gases. *Nat. Geosci.* **2**(8), 543.

Sherwood Lollar B., Lacrampe-Couloume G., Slater G. F., Ward J., Moser D. P., Gihring T. M. and Onstott T. C. (2006) Unravelling abiogenic and biogenic sources of methane in the Earth's deep subsurface. *Chem. Geol.* **226**(3), 328–339.

Shima S. and Thauer R. K. (2005) Methyl-coenzyme M reductase and the anaerobic oxidation of methane in methanotrophic Archaea. *Curr. Opin. Microbiol.* **8**(6), 643–648.

Shuai Y., Douglas P. M., Zhang S., Stolper D. A., Ellis G. S., Lawson M. and Hu G. (2018) Equilibrium and non-equilibrium controls on the abundances of clumped isotopologues of methane during thermogenic formation in laboratory experiments: implications for the chemistry of pyrolysis and the origins of natural gases. *Geochim. Cosmochim. Acta* **223**, 159–174.

Simkus D. N., Slater G. F., Lollar B. S., Wilkie K., Kieft T. L., Magnabosco C. and Sakowski E. G. (2016) Variations in microbial carbon sources and cycling in the deep continental subsurface. *Geochim. Cosmochim. Acta* **173**, 264–283.

Skuce M., Longstaffe F. J., Carter T. R. and Potter J. (2015) Isotopic fingerprinting of groundwaters in southwestern Ontario: applications to abandoned well remediation. *Appl. Geochem.* **58**, 1–13.

Stolper D. A., Sessions A. L., Ferreira A. A., Neto E. S., Schimmelmann A., Shusta S. S. and Eiler J. M. (2014a) Combined 13 C-D and D–D clumping in methane: methods and preliminary results. *Geochim. Cosmochim. Acta* **126**, 169–191.

Stolper D. A., Lawson M., Davis C. L., Ferreira A. A., Neto E. S., Ellis G. S. and Sessions A. L. (2014b) Formation temperatures of thermogenic and biogenic methane. *Science* **344**(6191), 1500–1503.

Stolper D. A., Martini A. M., Clog M., Douglas P. M., Shusta S. S., Valentine D. L. and Eiler J. M. (2015) Distinguishing and understanding thermogenic and biogenic sources of methane using multiply substituted isotopologues. *Geochim. Cosmochim. Acta* **161**, 219–247.

Stolper D. A., Lawson M., Formolo M. J., Davis C. L., Douglas P. M. and Eiler J. M. (2017) The utility of methane clumped isotopes to constrain the origins of methane in natural gas accumulations. *Geol. Soc. Lond. Special Publications* **468**, SP468-3.

Tang Y., Perry J. K., Jenden P. D. and Schoell M. (2000) Mathematical modeling of stable carbon isotope ratios in natural gases. *Geochim. Cosmochim. Acta* **64**(15), 2673–2687.

Thauer R. K. (2011) Anaerobic oxidation of methane with sulfate: on the reversibility of the reactions that are catalyzed by enzymes also involved in methanogenesis from CO_2. *Curr. Opin. Microbiol.* **14**(3), 292–299.

Timmers P. H., Welte C. U., Koehorst J. J., Plugge C. M., Jetten M. S. and Stams A. J. (2017) Reverse Methanogenesis and respiration in methanotrophic archaea. *Archaea* **2017**.

Tissot B. and Welte D. (1978) *Petroleum Formation and Occurrence: A New Approach to Oil and Gas Exploration*. Springer Science & Business Media.

Trevail, R. A., Carter, T. R. and McFarland, S. (2004) Trenton–Black River hydrothermal dolomite reservoirs in Ontario: an assessment of remaining potential after 100 years of production. In Proceedings 43rd Annual Conference Ontario Petroleum Institute Tec.

Valentine D. L., Chidthaisong A., Rice A., Reeburgh W. S. and Tyler S. C. (2004) Carbon and hydrogen isotope fractionation by moderately thermophilic methanogens. *Geochim. Cosmochim. Acta* **68**(7), 1571–1590.

Valentine D. L., Kessler J. D., Redmond M. C., Mendes S. D., Heintz M. B., Farwell C. and Chan E. W. (2010) Propane respiration jump-starts microbial response to a deep oil spill. *Science* **330**(6001), 208–211.

Vinson D. S., Blair N. E., Martini A. M., Larter S., Orem W. H. and McIntosh J. C. (2017) Microbial methane from in situ biodegradation of coal and shale: a review and reevaluation of hydrogen and carbon isotope signatures. *Chem. Geol.* **453**, 128–145.

Waldron P. J., Petsch S. T., Martini A. M. and Nüsslein K. (2007) Salinity constraints on subsurface archaeal diversity and methanogenesis in sedimentary rock rich in organic matter. *Appl. Environ. Microbiol.* **73**(13), 4171–4179.

Wang Zhengron, Schauble Edwin A. and Eiler John M. (2004) Equilibrium thermodynamics of multiply substituted isotopologues of molecular gases. *Geochim. Cosmochim. Acta* **68**(23), 4779–4797.

Wang D. T., Gruen D. S., Sherwood Lollar B., Hinrichs K. U., Stewart L. C., Holden J. F. and Delwiche K. B. (2015) Nonequilibrium clumped isotope signals in microbial methane. *Science* **348**(6233), 428–431.

Wang D. T., Welander P. V. and Ono S. (2016) Fractionation of the methane isotopologues $^{13}CH_4$, $^{12}CH_3$ D, and $^{13}CH_3D$ during aerobic oxidation of methane by Methylococcus capsulatus (Bath). *Geochim. Cosmochim. Acta* **192**, 186–202.

Wang D. T., Reeves E. P., McDermott J. M., Seewald J. S. and Ono S. (2018) Clumped isotopologue constraints on the origin of methane at seafloor hot springs. *Geochim. Cosmochim. Acta* **223**, 141–158.

Ward J. A., Slater G. F., Moser D. P., Lin L. H., Lacrampe-Couloume G., Bonin A. S. and Onstott T. C. (2004) Microbial hydrocarbon gases in the Witwatersrand Basin, South Africa: implications for the deep biosphere. *Geochim. Cosmochim. Acta* **68**(15), 3239–3250.

Webb M. A. and Miller, III, T. F. (2014) Position-specific and clumped stable isotope studies: comparison of the Urey and path-integral approaches for carbon dioxide, nitrous oxide, methane, and propane. *J. Phys. Chem. A* **118**(2), 467–474.

Whiticar M. J. (1999) Carbon and hydrogen isotope systematics of bacterial formation and oxidation of methane. *Chem. Geol.* **161**(1), 291–314.

Whiticar M. J., Faber E. and Schoell M. (1986) Biogenic methane formation in marine and freshwater environments: CO_2 reduction vs. acetate fermentation—isotope evidence. *Geochim. Cosmochim. Acta* **50**(5), 693–709.

Widdel F., Kohring G. W. and Mayer F. (1983) Studies on dissimilatory sulfate-reducing bacteria that decompose fatty acids. *Arch. Microbiol.* **134**(4), 286–294.

Wilson T. P. and Long D. T. (1993) Geochemistry and isotope chemistry of CaNaCl brines in Silurian strata, Michigan Basin, USA. *Appl. Geochem.* **8**(5), 507–524.

Wolin E. A., Wolin M. and Wolfe R. S. (1963) Formation of methane by bacterial extracts. *Journal of Biological Chemistry* **238**(8), 2882–2886.

Wuchter C., Banning E., Mincer T. J., Drenzek N. J. and Coolen M. J. (2013) Microbial diversity and methanogenic activity of Antrim Shale formation waters from recently fractured wells. *Front. Microbiol.*, 4.

Xia X. and Gao Y. (2017) Mechanism of linear covariations between isotopic compositions of natural gaseous hydrocarbons. *Org. Geochem.* **113**, 115–123.

Yeung L. Y. (2016) Combinatorial effects on clumped isotopes and their significance in biogeochemistry. *Geochim. Cosmochim. Acta* **172**, 22–38.

Young E. D., Rumble D., Freedman P. and Mills M. (2016) A large-radius high-mass-resolution multiple-collector isotope ratio mass spectrometer for analysis of rare isotopologues of O_2, N_2, CH_4 and other gases. *Int. J. Mass Spectrom.* **401**, 1–10.

Young E. D., Kohl I. E., Sherwood Lollar B., Etiope G., Rumble D., Li S. and Sutclife C. (2017) The relative abundances of

resolved $^{12}CH_2D_2$ and $^{13}CH_3D$ and mechanisms controlling isotopic bond ordering in abiotic and biotic methane gases. *Geochim. Cosmochim. Acta* **203**, 235–264.

Yoshinaga M. Y., Holler T., Goldhammer T., Wegener G., Pohlman J. W., Brunner B. and Elvert M. (2014) Carbon isotope equilibration during sulphate-limited anaerobic oxidation of methane. *Nat. Geosci.* **7**(3), 190–194.

Zhang T. and Krooss B. M. (2001) Experimental investigation on the carbon isotope fractionation of methane during gas migration by diffusion through sedimentary rocks at elevated temperature and pressure. *Geochim. Cosmochim. Acta* **65**(16), 2723–2742.

Zhilina T. N., Zavarzina D. G., Kevbrin V. V. and Kolganova T. V. (2013) Methanocalculus natronophilus sp. nov., a new alkaliphilic hydrogenotrophic methanogenic archaeon from a soda lake, and proposal of the new family Methanocalculaceae. *Microbiology* **82**(6), 698–706.

Associate editor: Edward Hornibrook